Neuron
NeuroResource

Permanent Genetic Access to Transiently Active Neurons via TRAP: Targeted Recombination in Active Populations

Casey J. Guenthner,[1,2,3] Kazunari Miyamichi,[1,2] Helen H. Yang,[3] H. Craig Heller,[2,3] and Liqun Luo[1,2,3,*]
[1]Howard Hughes Medical Institute
[2]Department of Biology
[3]Neurosciences Program
Stanford University, Stanford, CA 94305, USA
*Correspondence: lluo@stanford.ed
http://dx.doi.org/10.1016/j.neuron.2013.03.025

SUMMARY

Targeting genetically encoded tools for neural circuit dissection to relevant cellular populations is a major challenge in neurobiology. We developed an approach, targeted recombination in active populations (TRAP), to obtain genetic access to neurons that were activated by defined stimuli. This method utilizes mice in which the tamoxifen-dependent recombinase CreER^{T2} is expressed in an activity-dependent manner from the loci of the immediate early genes *Arc* and *Fos*. Active cells that express CreER^{T2} can only undergo recombination when tamoxifen is present, allowing genetic access to neurons that are active during a time window of less than 12 hr. We show that TRAP can provide selective access to neurons activated by specific somatosensory, visual, and auditory stimuli and by experience in a novel environment. When combined with tools for labeling, tracing, recording, and manipulating neurons, TRAP offers a powerful approach for understanding how the brain processes information and generates behavior.

INTRODUCTION

Our understanding of neural circuits has been greatly facilitated over the last decade by genetically encoded tools for visualizing neuronal structure and activity, manipulating neuronal function, and identifying synaptic connections. The application of these tools depends critically on the ability to target them to specific subpopulations of neurons on the basis of criteria such as cell type and location. For instance, one common strategy to express a tool in a particular cell type and brain region is to use local injections of Cre-dependent viruses into genetically engineered mice that express Cre recombinase in a specific cell type (Zhang et al., 2010). Other strategies allow neurons to be targeted on the basis of a variety of anatomical, genetic, and developmental criteria (Luo et al., 2008). However, in many cases, considerable functional heterogeneity exists within neuronal populations that are anatomically, developmentally, and genetically indistinguishable by current methods. For instance, neurons tuned to differently oriented visual stimuli are intermingled in the rodent primary visual cortex (Ohki et al., 2005), neurons that are activated by different odorants are distributed randomly in the mouse piriform cortex (Stettler and Axel, 2009), and neurons activated during fighting or mating in mice are intermingled in multiple brain areas (Lin et al., 2011). Even neuronal representations previously thought to be anatomically organized, such as tonotopically arranged frequency representations in the auditory cortex, are now known to be disordered at a fine scale (Rothschild et al., 2010). The ability to have genetic access to such functionally similar but spatially distributed and genetically indistinct neuronal populations would significantly advance our ability to investigate neural circuits underlying sensory experience and behavior.

Immediate early genes (IEGs) are the most well-studied connection between gene expression and a neuron's electrical and/or synaptic activity, which defines its response properties. Exploiting this connection is a promising strategy for gaining genetic access to active neuronal populations. IEG expression is low in quiescent cells but can be induced rapidly and transiently by external stimuli. For example, the expression of the prototypical IEG *Fos* can be induced in vitro by growth factors and neurotransmitters and in vivo by neuronal and synaptic activity, as well as by physiological stimuli (reviewed by Sheng and Greenberg, 1990). The products of many IEGs, including *Fos*, are transcription factors that regulate cellular function through downstream transcriptional programs, but others can directly influence neuronal function. For instance, activity-regulated cytoskeleton-associated protein (*Arc*) is an IEG that encodes a postsynaptically localized protein that directly influences synaptic function (Lyford et al., 1995). *Fos*, *Arc*, and other IEGs have been frequently used as markers for neurons that were active during a short period prior to sacrifice. Although no single IEG is a perfect surrogate for neuronal activity, throughout this paper, we use "activity" loosely to refer to IEG expression.

Activity-dependent IEG expression has been exploited in a number of methods for studying neural circuits. With these methods, it is possible to identify cells that express IEGs in response to multiple stimuli separated in time (Guzowski et al.,

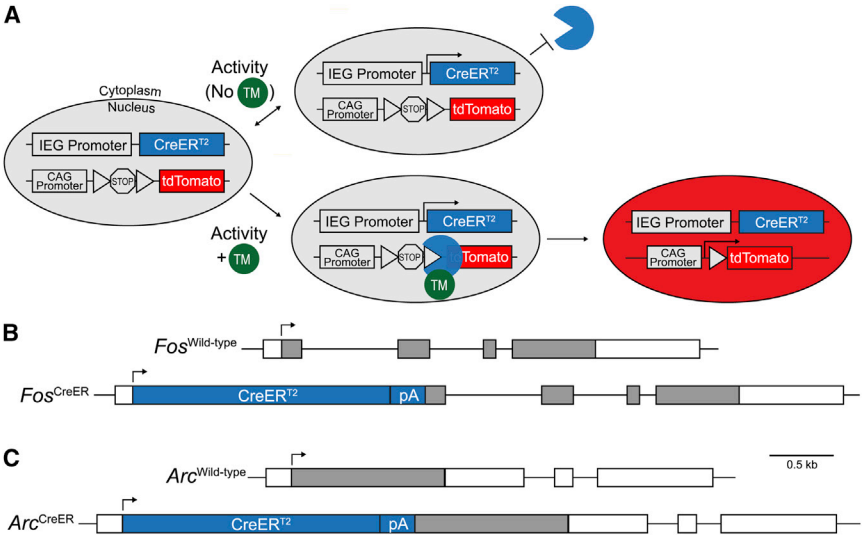

Figure 1. Strategy of TRAP, Targeted Recombination in Active Populations

(A) TRAP requires two transgenes: one that expresses CreER^{T2} from an activity-dependent IEG promoter and one that allows expression of an effector gene, such as tdTomato, in a Cre-dependent manner. Without tamoxifen (TM), CreER^{T2} is retained in the cytoplasm of active cells in which it is expressed, so no recombination can occur (top). In the presence of TM, CreER^{T2} recombination can occur in active cells (bottom), whereas nonactive cells do not undergo recombination, because they do not express CreER^{T2}.

(B and C) Schematics of the wild-type and CreER^{T2} knockin alleles of *Fos* (B) and *Arc* (C). Rectangles indicate exons, and protein-coding regions are shaded gray. Arrows indicate translational start sites.

See also Figure S1.

1999), visualize active neurons in fixed or live tissue from transgenic animals (Barth et al., 2004; Smeyne et al., 1992; Wang et al., 2006), and manipulate the activities of IEG-expressing populations (Garner et al., 2012; Koya et al., 2009; Liu et al., 2012; Reijmers et al., 2007). Although these strategies have been useful for addressing many biological questions, they suffer from a number of limitations, including poor temporal resolution, transience of effector protein expression, and low signal-to-noise ratio. Here, we describe an approach using genetically engineered mice to obtain permanent genetic access to distributed neuronal populations that are activated by experiences within a limited time window. This approach, called targeted recombination in active populations (TRAP), offers several advantages over currently available technologies and, when combined with genetically encoded effectors for visualizing and manipulating neurons, has the potential to greatly facilitate experimental dissection of neural circuit function.

RESULTS

Strategy for Genetically Accessing Neuronal Populations on the Basis of Immediate Early Gene Expression

TRAP utilizes two genetic components: (1) a transgene that takes advantage of IEG regulatory elements in order to express a drug-dependent recombinase, such as the tamoxifen (TM)-dependent Cre recombinase CreER^{T2} (Feil et al., 1997), in an activity-dependent manner and (2) a transgene or virus that expresses an effector protein in a recombination-dependent manner (Figure 1A). For the first component, we generated knockin mice in which CreER^{T2} is expressed from the endogenous *Fos* and *Arc* loci (Figure 1B and Figure S1 available online). These knockins retain all sequences 5′ to the translational start site but replace the endogenous 3′ untranslated regions (3′UTRs), which contribute to messenger RNA (mRNA) destabilization and *Arc* mRNA dendritic trafficking (see Supplemental Experimental Procedures), with an exogenous SV40 polyadenylation signal to promote high-level expression. The introns and coding regions are also displaced (Figures 1B and S1). Although these alleles are predicted to be null for *Arc* and *Fos*, we have not observed any gross behavioral or anatomical abnormalities in the resulting heterozygous *Arc*$^{CreER/+}$ and *Fos*$^{CreER/+}$ mice (see Discussion). For the second component, we used AI14, a knockin allele of the *Rosa26* (*R26*) locus that allows high-level ubiquitous expression of the red fluorescent protein tdTomato after the excision of a loxP-flanked transcriptional stop signal (Madisen et al., 2010).

In the absence of TM, CreER^{T2} is retained in the cytoplasm of active cells and no recombination can occur (Figure 1A, top). TM administration causes active CreER^{T2}-expressing cells to undergo Cre-mediated recombination (to be "TRAPed"), resulting in permanent expression of the effector gene (e.g., tdTomato; Figure 1A, bottom). Nonactive cells do not express CreER^{T2} and do not undergo recombination, even in the presence of TM. Because of the transient nature of IEG transcription, CreER^{T2} is only present for a limited time after neuronal activation, and the lifetime of TM is limited by metabolism and excretion; as a result, only neurons that are active within a limited time window around drug administration can be TRAPed.

Background Recombination Is Very Low in FosTRAP Mice and Is Limited to Specific Cell Types in ArcTRAP Mice

Because many CreER^{T2} lines have drug-independent recombination as a result of leaky CreER^{T2} activity (e.g., Madisen et al., 2010), we first examined recombination in FosTRAP (*Fos*$^{CreER/+}$ *R26*$^{AI14/+}$) and ArcTRAP (*Arc*$^{CreER/+}$*R26*$^{AI14/+}$) mice that were not treated with TM. Under these conditions, we observed very few labeled cells (from zero to a few cells per 60 μm sagittal section) in both young adult (Figures 2A, top, and 2C, left column) and aged (6- to 7-month-old; Figures S2B, top, and S2C, right column) FosTRAP mice. Thus, despite CreER^{T2} expression in response to neuronal activity throughout the life of the animal, cytoplasmic retention of the CreER^{T2} protein in the absence of TM prevented CreER^{T2}-induced recombination (Figure 1A, top). Labeling in untreated ArcTRAP mice is significant but is

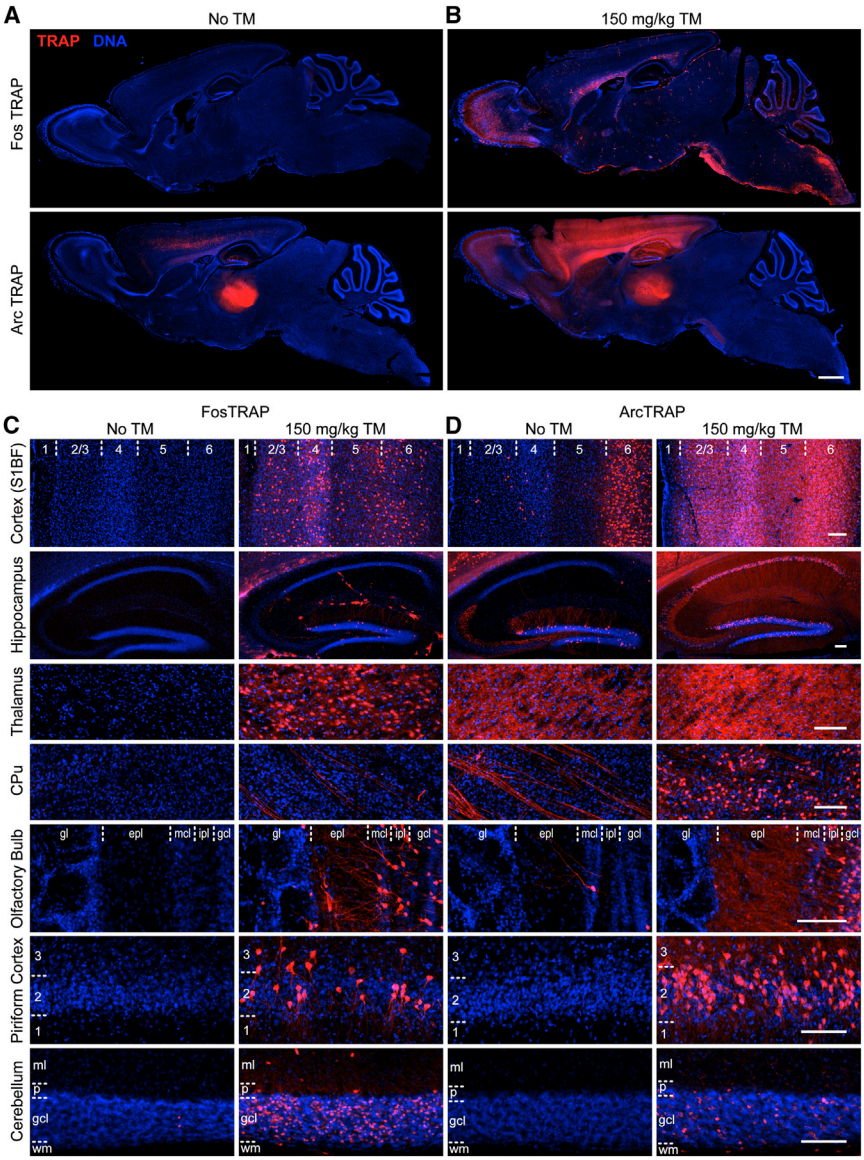

Figure 2. Background and Homecage Recombination in FosTRAP and ArcTRAP Mice

(A and B) Full sagittal views of FosTRAP (top) and ArcTRAP (bottom) brains from 6- to 8-week-old mice that were either uninjected (A) or treated with TM in the homecage and sacrificed 1 week post-injection (B). The scale bar represents 1 mm.

(C and D) Magnified views from uninjected (left columns) or homecage TM-treated (right columns) FosTRAP (C) and ArcTRAP (D) brains. Images are representative of at least n = 3 mice examined per condition. The thalamus images are of the ventral posteromedial (VPM) thalamus, a somatosensory thalamic nucleus. S1BF, primary somatosensory barrel field; CPu, caudate putamen; gl, glomerular layer; epl, external plexiform layer; mcl, mitral cell layer; ipl, internal plexiform layer; gcl, granule cell layer; ml, molecular layer; p, Purkinje cell layer; and wm, white matter. Numbers indicate cortical layers. The scale bar represents 100 μm.

See also Figure S2.

restricted to a few specific cell types, including layer 6 neurons in neocortex and granule cells in the dentate gyrus (DG; Figures 2A, bottom, and 2D, left column). The TM-independent recombination in ArcTRAP mice is most likely caused by *Arc*'s relatively high level of expression (Lyford et al., 1995). Consistent with this assumption, the frequency of labeled cells in untreated ArcTRAP mice increased with the animal's age (Figures S2B, bottom, and S2D, right column). The remaining experiments in this paper were performed in mice that were 6–8 weeks of age.

Fos and *Arc* Loci Drive CreER Activity in Partially Overlapping Neuronal Populations in the Homecage

Treatment of both FosTRAP and ArcTRAP mice with TM (150 mg/kg intraperitoneal [i.p.] injected) in the homecage induced labeling in restricted regions throughout the brain when mice were examined 1 week postinjection (Figures 2B and 2C–2D, right columns). Because tdTomato fills cell bodies and processes, the identities of recombined cells could readily be determined by morphology. In FosTRAP mice, we observed recombination in cells lining the brain and ventricle surfaces, in blood vessels, and in putative oligodendrocytes in white matter. Within the gray matter, recombination occurred almost exclusively in cells with neuronal morphologies; recombination in gray matter glial cells was rarely observed. In ArcTRAP mice, TM treatment induced labeling most dramatically in forebrain regions and was exclusively neuronal. In comparison to uninjected controls, mice injected with vehicle showed no increase in the numbers of labeled cells in either line, indicating that the stimulus of injection alone was insufficient to trigger recombination in the absence of TM (Figures S2A and S2C and S2D, left columns).

Following homecage TM treatment, ArcTRAP and FosTRAP mice had similar patterns of recombination in many brain areas (Figures 2C–2D, right columns), including in neocortex, where labeled cells were relatively sparse in layer 5; in the hippocampus, where labeled cells were enriched in the DG and in CA1; in the piriform cortex; and in the olfactory bulb, where granule cells were heavily TRAPed. Even for those cell types that had high background recombination in untreated ArcTRAP mice, TM treatment increased labeling (e.g., compare the left and right columns in Figure 2D for the hippocampus and neocortical layer 6). In most brain regions, the recombination frequency was higher in ArcTRAP mice than in FosTRAP mice, but FosTRAP was more efficient in some areas, such as the cerebellum. In the thalamus of ArcTRAP mice, no recombination in intrinsic thalamic neurons was detected despite the presence of densely

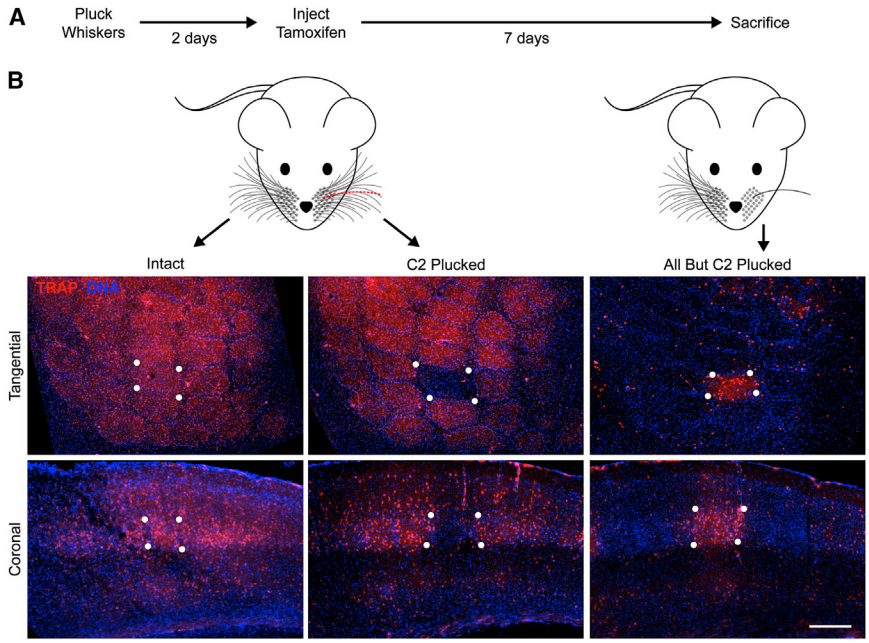

Figure 3. FosTRAP in the Barrel Cortex of Whisker-Plucked Mice

(A) Experimental scheme: FosTRAP mice had either all whiskers except C2 plucked unilaterally or had only the C2 whisker plucked. After a 2 day recovery period, mice were injected with 150 mg/kg TM, and recombination was examined 7 days later.

(B) Tangential views of flattened layer 4 of the primary somatosensory barrel cortex (top) or coronal views through the C2 barrel (bottom). White dots indicate the corners of the C2 barrel on the basis of dense DAPI staining of the barrel walls. Compared with controls (left), removal of only the C2 whisker results in elimination of TRAP signal from the C2 barrel (middle), whereas removal of all whiskers except C2 results in absence of most TRAPed cells in all barrels except C2 (right). The left and middle images are from the same mouse. Images are representative of at least 3–4 mice for each condition. The scale bar represents 250 μm. See also Figure S3.

labeled corticothalamic axons. In contrast, FosTRAP mice showed efficient recombination in some thalamic nuclei. On the other hand, medium spiny neurons of the striatum were efficiently labeled with ArcTRAP, but not with FosTRAP.

The high frequency of recombination under homecage conditions in both FosTRAP and ArcTRAP mice contrasts with the low levels of *Fos* and *Arc* expression under similar conditions (Lyford et al., 1995; Morgan et al., 1987). Given that CreER^{T2}-mediated recombination is irreversible, TRAPed cells accumulate as long as TM is present; in addition, perdurance of CreER^{T2} mRNA or protein may allow TRAPing of cells activated prior to TM injection. Thus, the final TRAPed population is a result of activity integrated over a time window determined by CreER^{T2} stability and TM metabolism and excretion. In contrast, endogenous Arc and Fos are rapidly degraded after induction and, thus, report activity over a more limited time period prior to sacrifice.

The above experiments demonstrate that, with the exception of a small subset of cell types in the ArcTRAP mice, recombination in TRAP mice is TM dependent. They also show that *Arc* and *Fos* loci differ to some extent in their cell-type specificities. Finally, although ArcTRAP has higher background recombination than FosTRAP, it also has higher TM-induced recombination (compare the bottom panels of Figures 2A and 2B). Thus, the two lines may be preferred for certain types of experiments depending on the relative importance of specificity versus efficiency and the cell types of interest.

Recombination in the Primary Somatosensory Cortex Is Dependent on Sensory Input

To determine whether neurons that are activated by specific sensory stimuli can be TRAPed, we performed sensory deprivation experiments in the whisker-barrel system of TRAP mice. Somatosensory information from the facial vibrissae are relayed via brainstem and thalamic nuclei to contralateral primary somatosensory cortex (S1) where thalamic afferents representing individual whiskers innervate discrete somatotopically organized "barrels" in layer 4 (Petersen, 2007). Stimulation of a single whisker induces IEG expression selectively in the corresponding barrel (Staiger et al., 2000). Below, we describe results on FosTRAP mice (Figure 3); however, qualitatively similar results were obtained with ArcTRAP (Figure S3).

After manipulating sensory input to the barrel cortex by plucking specific whiskers, we injected mice with TM and returned them to the homecage with tubes and nesting material to stimulate whisker exploration (Figure 3A). When all whiskers were left intact, labeled processes and cells were distributed uniformly across all barrels (Figure 3B, left), which were visible both in coronal sections (Figure 3B, bottom) and in sections tangential to layer 4 (Figure 3B, top). In contrast, when all large whiskers except C2 were plucked, a dense collection of cells and processes was apparent in the C2 barrel, with only scattered labeled cells present in other barrels (Figure 3B, right). This restriction of labeled cells to the C2 barrel extended up to layers 2/3, but not down to layer 6, where a large number of cells outside the C2 barrel were labeled (Figure 3B, right). Thus, TRAPing of cells in the barrel cortex is dependent on specific sensory input.

Layer 4 barrel neurons can be activated by deflections of adjacent whiskers (Armstrong-James et al., 1992). To test the contributions of these nonprincipal inputs to TRAPing, we repeated the above experiment in mice that had only the C2 whisker removed. We found that, under these conditions, the corresponding C2 barrel was devoid of labeled cells and processes and that this effect was strongest in layer 4 (Figure 3B, middle). This observation suggests that *Fos* expression in layer 4 is evoked mainly by thalamocortical input, either directly by thalamocortical synapses or indirectly by intracortical connections within a barrel.

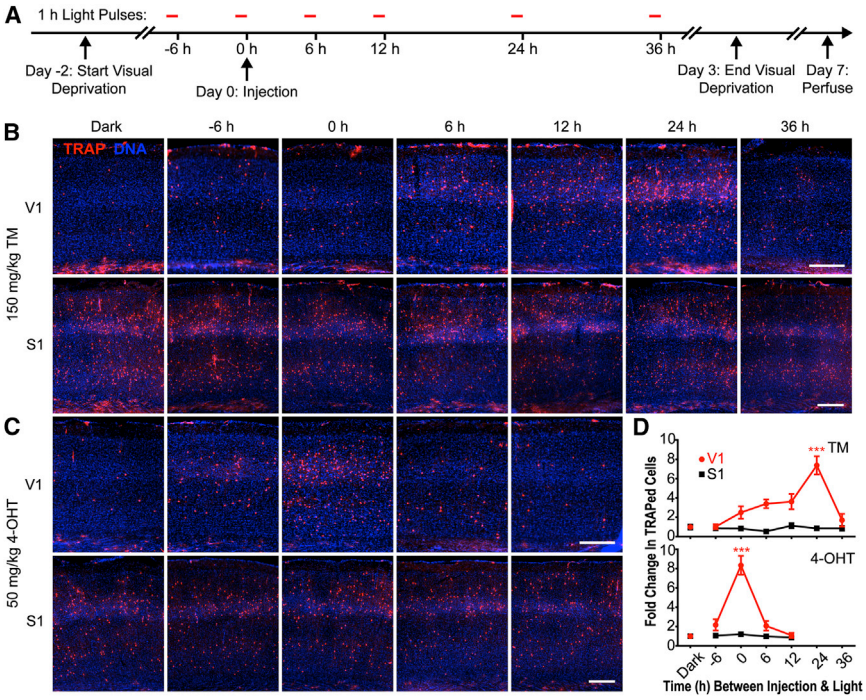

Figure 4. Time Window for Effective TRAPing Relative to Drug Injection in Primary Visual Cortex

(A) Experimental scheme: FosTRAP mice were placed in constant darkness for 2 days and were then given injections of either 150 mg/kg TM or 50 mg/kg 4-OHT at varying times relative to a 1 hr diffuse light stimulus. Mice remained in darkness for three days after drug injection and were sacrificed 7 days later.

(B and C) Representative images of primary visual (V1, top rows) and somatosensory (S1, bottom rows) cortices in mice treated with TM (B) or 4-OHT (C) at different times relative to the light stimulus. The scale bar represents 250 μm.

(D) Quantification (mean ± SEM, n = 4–7 mice per time point) of the density of TRAPed cells in V1 and S1 normalized to the mean density of TRAPed cells in the dark condition for both TM (top) and 4-OHT (bottom). In S1 of mice treated with either drug, light stimulation did not increase the number of TRAPed cells over dark levels (ANOVAs, $p > 0.3$). For V1, the window for TRAPing was longer and had a later peak for TM than for 4-OHT. ***, significantly different from the dark condition for V1 ($p < 0.001$, Tukey's post hoc test after significant ANOVA). All other time points were not significantly different from dark ($p > 0.05$). See also Figures S4 and S5.

Different Forms of Tamoxifen Allow Activity to Be TRAPed Over Different Time Windows

We performed additional characterization of TRAP in the visual system, where IEG expression can be robustly induced by light (Kaczmarek and Chaudhuri, 1997), focusing on FosTRAP because of its low TM-independent background. Light stimulation increased the numbers of TRAPed cells in the dorsal lateral geniculate nucleus (dLGN) and primary visual cortex (V1) by 4.2- and 8.3-fold, respectively, relative to mice maintained in the dark (Figures 4 and S4A–S4C). The TRAPed cells were distributed across all layers of V1 but were most dense in layer 4, and more than 96% of the TRAPed cells expressed the neuronal marker NeuN; the remaining ~4% of cells included putative endothelial cells and glia (Figure S4E). Fewer than ~3% of V1 cells were GABAergic (Figure S4E). Thus, most TRAPed cells in V1 are excitatory neurons.

To determine the time window around a TM injection during which active cells are efficiently TRAPed, we examined V1 in FosTRAP mice that had been stimulated with 1 hr of diffuse bright light at various times relative to the injection (Figure 4A). TRAPing was maximal when light stimulation occurred 23–24 hr after injection. No TRAPing above the level of the dark control occurred when light was given 6–7 hr before the injection or 35–36 hr after injection (Figures 4B and 4D). Labeling in a control region (S1) was similar across all time points (Figures 4B and 4D). Thus, under these conditions, TRAP appears to be sensitive to neuronal activation that occurs less than 6 hr prior to injection and up to 24–36 hr after injection.

A long time window may be desirable in cases where it is beneficial to TRAP cells on the basis of the integration of activity over a long period of time. However, applications that utilize stimuli and experiences of short duration could benefit from a shorter time window. After injection, TM is metabolized to its principal active form, 4-hydroxytamoxifen (4-OHT; Robinson et al., 1991). Directly injecting 4-OHT shortened the TRAPing time window to <12 hr (Figure 4D); optimal TRAPing in V1 was observed when light was administered in the hour immediately before injection of 4-OHT, and minimal TRAPing was observed when light was delivered 6–7 hr before or 5–6 hr after the injection.

To determine the dependence of TRAP on stimulus duration, we delivered light pulses of varying durations beginning 1 hr before a 4-OHT injection. Relative to mice left in the dark, mice exposed to light pulses of 5, 15, and 60 min in duration had 2.6-, 4.9-, and 8.3-fold more TRAPed cells in V1 (Figures S5A–S5C). Thus, even short (5 min) stimuli are sufficient for TRAPing, although longer duration stimuli increase the total numbers of TRAPed cells. These results are consistent with prior findings that the induction of Fos protein in V1 is dependent on stimulus duration (Amir and Robinson, 1996).

The time course of effector expression after TRAPing determines the earliest time point at which subsequent experimental manipulations are possible. Although this parameter is most likely to be dependent on effector and cell type, we found that it took at least 72 hr following light stimulation and 4-OHT injection for TRAPed V1 cells to express sufficiently high levels of tdTomato to be reliably identified (Figures S5D–S5F).

TRAP Provides Selective Genetic Access to Cochlear Nucleus Neurons Tuned to Specific Sound Frequencies

Next, we took advantage of the tonotopic organization of the auditory system to evaluate whether TRAP can provide genetic access to cell populations that are activated by particular features of sensory stimuli. We focused on the cochlear nucleus (CN), all three subdivisions of which receive input from spiral

ganglion neurons (SGNs) that carry auditory information from the cochlea. SGNs that innervate the apex or the base of the cochlea are tuned to low- and high-frequency sounds and terminate their axons in the ventral or dorsal regions of each CN subdivision, respectively. Thus, SGN axons are arrayed in a high-to-low-frequency tonotopic map along the dorsoventral axis of the CN (Young and Oertel, 2004). Similar tonotopy is observed in CN neuronal responses themselves, determined both electrophysiologically (Luo et al., 2009) and by *Fos* induction (Friauf, 1992; Saint Marie et al., 1999).

We injected FosTRAP mice with 4-OHT during a 4 or 16 kHz continuous pure tone stimulus to TRAP CN neurons tuned to those frequencies. To increase the total number of TRAPed cells, we took advantage of TRAP's ability to integrate IEG expression over time by using a 4 hr pure tone stimulus during the TRAPing period. Then, 4–5 days later, we delivered a second 4 or 16 kHz stimulus for 1 hr, sacrificed the mice 1 hr later, and processed the tissue for Fos immunostaining (Figure 5A). Thus, TRAPed cells represent neurons activated by the first stimulus, and Fos protein immunopositive (Fos+) cells represent neurons activated by the second stimulus.

Consistent with prior results, we found that 4 kHz stimulation during the second epoch induced Fos expression in clusters of cells in all three CN subdivisions that were located more ventrally than the clusters that were Fos+ after 16 kHz stimulation. Similar results were observed for TRAPed cells. When the tone frequency was the same for the two stimulus epochs, the TRAPed and Fos+ populations overlapped, and the 4 kHz cluster was localized more ventrally than the 16 kHz cluster (Figure 5B, first and third columns). Within mice receiving stimuli of two different frequencies, the cells TRAPed by the 16 kHz stimulus were dorsal to Fos+ cells induced by the 4 kHz stimulus (Figure 5B, second column), whereas the reverse was true when the 4 kHz stimulus was TRAPed and the 16 kHz representation was revealed by Fos immunostaining (Figure 5B, last column). These qualitative impressions were confirmed by the quantification of the numbers of TRAPed and Fos+ cells in bins spanning the dorsoventral axis of the central dorsal cochlear nucleus (DCN; Figure 5C). In general, the populations of TRAPed cells were less sharply confined along the dorsoventral axis than the population of Fos+ cells. This may reflect the longer stimulus used for TRAPing (4 hr, versus 1 hr for Fos immunostaining) or some general noise in the TRAP approach. Regardless, this analysis supports the observations from individual sections that both TRAP and Fos immunostaining reveal similar tonotopic maps along the dorsoventral axis of the DCN.

We also quantified the overlap between TRAPed and Fos+ cells for the different treatment groups across the entire extent of the DCN. As expected, the overlap between the two populations was greater when the stimuli during the two epochs were the same (4kHz-4kHz and 16kHz-16kHz groups) than when the stimuli during the two epochs were different (16kHz-4kHz and 4kHz-16kHz groups; Figure 5D). The partial overlap in the 16kHz-4kHz and 4kHz-16kHz groups was not unexpected, given the complexity of the tuning curves for some types of CN neurons (Luo et al., 2009; Young and Oertel, 2004). The fact that ~70% of Fos+ cells were also TRAPed in the 16kHz-16kHz and 4kHz-4kHz groups (Figure 5D, left) suggests that TRAP can provide genetic access to the majority of cells that express Fos in response to a particular stimulus. Our finding that only ~30%–40% of TRAPed cells were Fos+ in these groups (Figure 5D, right) could be due to some noise intrinsic to the TRAP approach or to greater sensitivity of TRAP relative to Fos immunostaining; alternatively, it could be due to the TRAPing of cells that expressed Fos in response to the long-duration stimulus used during the TRAPing period but that did not express Fos in response to the shorter stimulus delivered prior to sacrifice.

Neurons Activated by Complex Experiences Can Be Effectively TRAPed

Although the experiments in the somatosensory, visual, and auditory systems suggest that TRAP can have high signal-to-noise ratio in the context of sensory deprivation and controlled stimulation, we wanted to evaluate whether it would also be possible to TRAP neurons activated by complex experiences. To this end, we allowed FosTRAP mice to explore a novel environment for 1 hr, injected them with either 4-OHT or vehicle, and allowed them to continue exploring the novel environment for another 1 hr. An additional group of mice received 4-OHT injections in the homecage. Mice were sacrificed 1 week after treatment. Virtually no cells were TRAPed in any brain region in mice given an injection of vehicle during novel environment exploration (Figures 6A and S6A), confirming that CreER activity is tightly regulated by tamoxifen. In comparison to 4-OHT-injected homecage controls, mice injected with 4-OHT in a novel environment had more TRAPed cells throughout the brain. For instance, novel environment exploration increased the numbers of TRAPed cells in piriform and barrel cortices by 1.9- and 3.5-fold, respectively (Figure S6), consistent with prior studies using in situ hybridization or immunohistochemistry to detect IEGs (Hess et al., 1995; Staiger et al., 2000). Interestingly, the TRAPing of oligodendrocytes in the white matter was not affected by novel environment exposure (Figure S6), suggesting that the differences in neuronal TRAPing were not due to variability in 4-OHT dosing or metabolism.

We also found that exploration of the novel environment increased the numbers of TRAPed DG granule cells and CA1 pyramidal cells by 2.4- and 2.9-fold, respectively, in comparison to homecage controls (Figure 6). This result is consistent with previous work using in situ hybridization to detect IEGs (Guzowski et al., 1999; Hess et al., 1995). TRAPed cells in CA3 were very sparse in all conditions. In the DG, more TRAPed cells were located in the upper (suprapyramidal) blade than in the lower (infrapyramidal) blade (Figure 6C). The increased TRAPing of DG granule cells with novel environment exploration was also greater in the upper blade than in the lower blade (Figure 6C), consistent with prior reports of an upper-blade-selective increase in *Arc* expression in rats exploring a novel environment (Chawla et al., 2005). Although the significance of this apparent functional difference between upper and lower blades is unclear, our data, along with prior results, suggest that it is consistent for different IEGs and across rats and mice. Moreover, TRAP can capture patterns of DG activity consistent with those obtained with classical methods, and TRAP has a sufficient signal-to-noise ratio in the absence of sensory deprivation to detect neuronal activity associated with complex experiences.

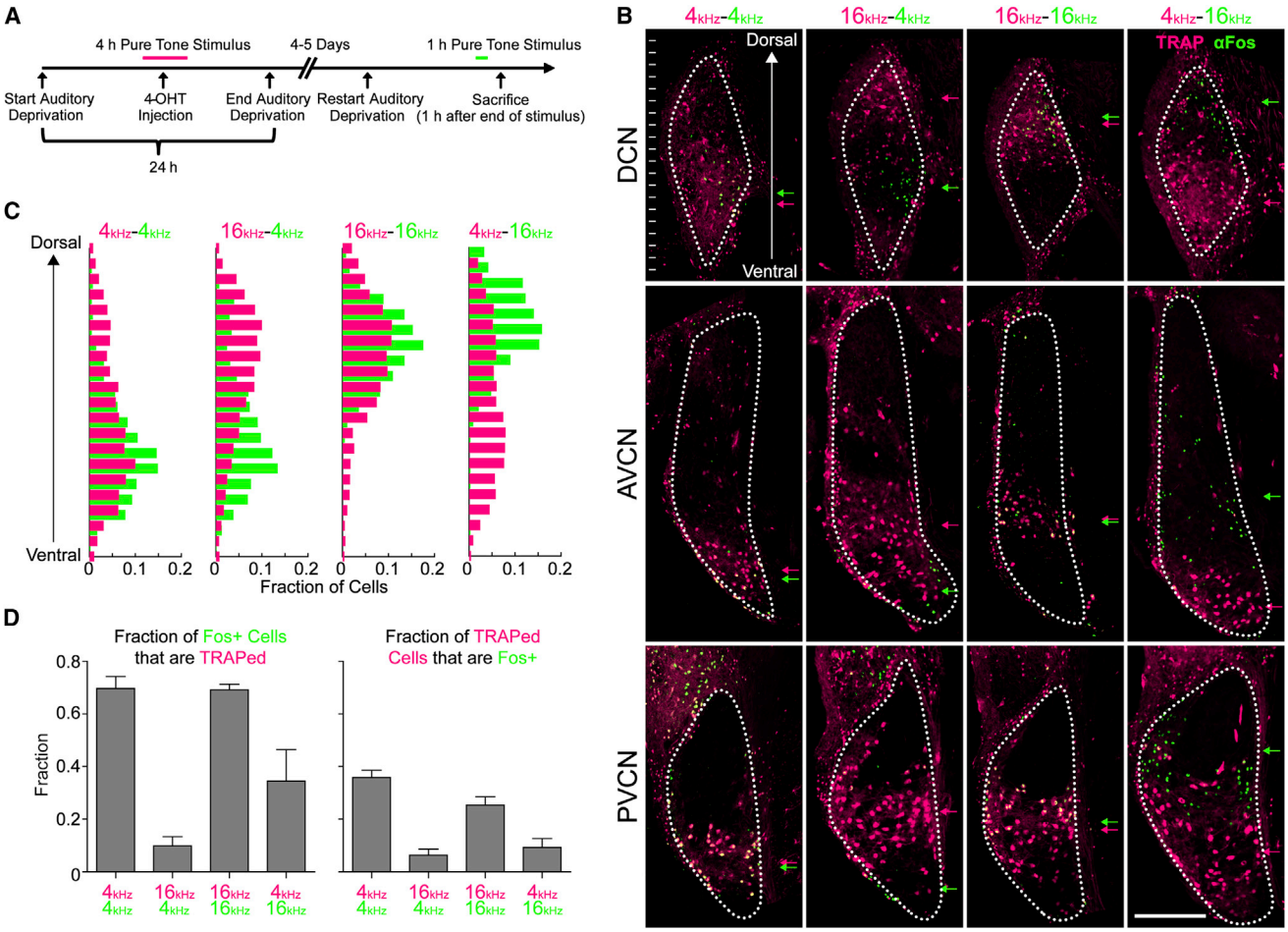

Figure 5. TRAPing Cells that Respond to Specific Frequencies of Auditory Stimuli

(A) Experimental scheme: FosTRAP mice were placed in a sound isolation chamber for 24 hr, during which they received a 4 hr pure tone stimulus (magenta bar). In the middle of the stimulus, they were injected with 50 mg/kg 4-OHT. Then, 4–5 days later, they were returned to the sound isolation chambers, where they received a 1 hr pure tone stimulus (green bar) ending 1 hr before they were sacrificed.

(B) Exemplary images of the dorsal, anteroventral, and posteroventral cochlear nuclei (DCN, AVCN, and PVCN, respectively), the cores of which are outlined with white dots on the basis of a DNA counterstain (data not shown). Fos immunostaining is shown in green, and magenta shows tdTomato fluorescence from TRAP. For the group names above each column, the frequencies represented by the TRAPed and Fos+ cells are indicated in magenta and green, respectively. Magenta and green arrows indicate the qualitative centers of TRAPed and Fos+ cell clusters, respectively, within each subdivision. The CN borders include granule cells that receive extensive nonauditory input (Young and Oertel, 2004) and that are thus TRAPed independently of the delivered stimulus. Similar results were observed in all 3–4 mice in each group. The scale bar represents 250 μm.

(C) Quantification of tonotopy in the DCN. Sections from the middle third of the rostrocaudal extent of the DCN were separated into bins along the dorsoventral axis (shown in the upper left panel in B), and the numbers of TRAPed (magenta histogram) and Fos+ (green histogram) cells (excluding granule cells) were counted for each bin and pooled across sections and animals. Total cell counts are 300–700 for the each of the Fos+ (green) histograms and 800–1,500 for each of the TRAP (magenta) histograms. Regardless of whether the neuronal representation was measured by Fos immunostaining or by TRAP, the higher-frequency tone activated cells localized more dorsally than the lower-frequency tone.

(D) Quantification (mean ± SEM, n = 3–4 mice per condition) of colabeling between TRAP and Fos immunostaining. For both plots, all groups were significantly different from each other (Tukey's post hoc tests, $p < 0.05$ after ANOVA, $p < 0.001$), except for 4kHz-4kHz versus 16kHz-16kHz and 16kHz-4kHz versus 4kHz-16kHz ($p > 0.05$).

DISCUSSION

Targeting genetically encoded effectors to relevant neuronal populations is a key step in many experiments aimed at deciphering how the brain processes information and generates behavior. Although neurons have traditionally been targeted on the basis of anatomical, developmental, or genetic criteria, TRAP allows neurons to be targeted on the basis of a functional criterion: whether or not they are activated by particular stimuli or experiences.

Applications of TRAP and Comparison to Other Approaches

Although the experiments reported here utilized a fluorescent protein as a reporter for TRAPed neurons, our *Fos*^{CreER} and *Arc*^{CreER} knockin alleles can be combined with different

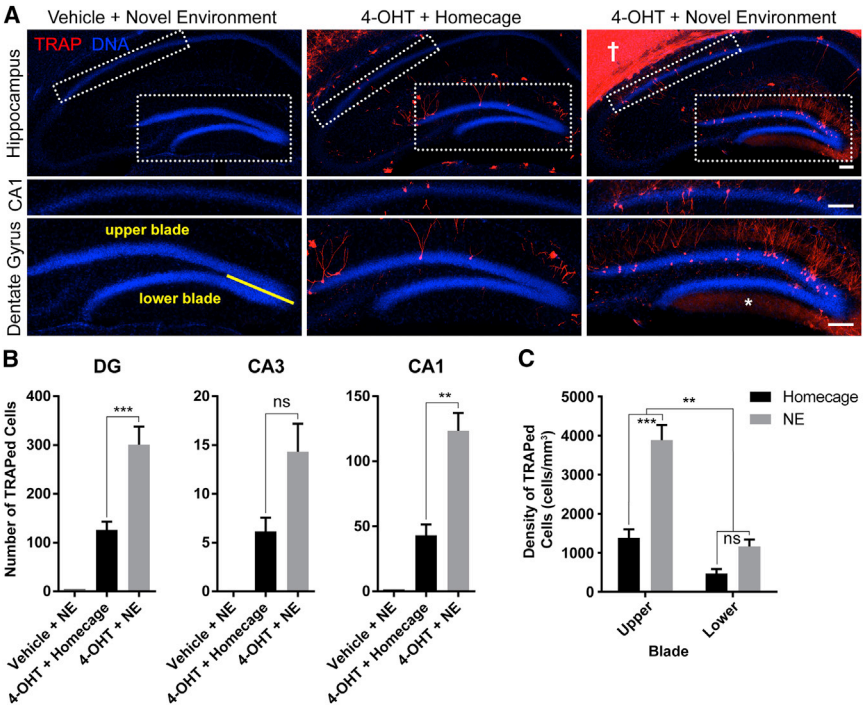

Figure 6. TRAPing Cells Activated by the Exploration of a Novel Environment

(A) Representative images of the hippocampus from FosTRAP mice that were injected with vehicle or 50 mg/kg 4-OHT while exploring a novel environment for 2 hr (left and right, respectively) or with 50 mg/kg 4-OHT in the homecage (middle). Mice were sacrificed 1 week after injection. Higher-magnification images of CA1 (middle) and the DG (bottom) correspond to the boxed regions in the top row. Virtually no cells were TRAPed in the vehicle-injected mice. In 4-OHT-injected mice, exploration of a novel environment led to an increase in TRAPed DG granule and CA1 pyramidal cells in comparison to mice left in the homecage. In the DG, TRAPed cells were located mostly in the upper (suprapyramidal) blade, indicated in the lower left panel as the region above the yellow line bisecting the genu. The highly TRAPed region in the upper right panel (†) is the barrel cortex (see Figure S6). TRAPing of cells with axons innervating the DG also increases with novel environment exposure, as indicated by the increase in diffuse tdTomato labeling of the DG molecular layer (*). The scale bar represents 100 μm.

(B) Quantification (mean ± SEM) of numbers of TRAPed DG granule cells and CA3 and CA1 pyramidal cells in mice treated with 4-OHT in the homecage (n = 6) or during the exploration of a novel environment (n = 6) or in mice treated with vehicle while exploring a novel environment (n = 3). Cell counts represent the total numbers of cells observed on one side of the hippocampus in every fourth coronal section across all but the most caudal portion of the hippocampus. Novel environment exploration significantly increased the numbers of TRAPed DG granule cells and CA1 pyramidal cells (***, $p < 0.001$; **, $p < 0.01$; Tukey's post hoc test after a significant two-way ANOVA with brain region and treatment as factors; statistical results for the vehicle controls were not determined because of the small number of cells observed in that condition).

(C) Quantification (mean ± SEM) of density of TRAPed DG granule cells in the upper and lower blades of the DG in mice treated with 4-OHT in the homecage or while exploring a novel environment (***, $p < 0.001$, Tukey's post hoc test; **, $p < 0.01$, blade X treatment interaction by two-way ANOVA).

See also Figure S6.

Cre-dependent transgenes or viruses in order to express a wide range of different effectors in TRAPed cells. This modular design will enable genetic manipulation of the TRAPed population for visualizing structure (with fluorescent proteins), recording activity (with genetically encoded calcium indicators), identifying synaptic connections (with genetically targeted viral transsynaptic tracers), or manipulating activity (with optogenetic and pharmacogenetic effectors).

Labeling Neurons Activated by a Single Experience

Detection of IEG expression by immunostaining or in situ hybridization enables high-resolution, whole-brain identification of neurons activated in unrestrained animals by experiences that occur within a limited time window before sacrifice. The development of transgenic animals and viruses that express fluorescent reporters from IEG-regulatory elements has allowed IEG-expressing neurons to be studied in live animals and tissues (Barth et al., 2004; Kawashima et al., 2009; Wang et al., 2006). With TRAP, effector proteins can be expressed from a strong promoter, enabling higher-level expression than is likely to be achieved by direct expression from activity-dependent elements. Thus, TRAP can facilitate experiments where strong labeling is important, such as whole-brain imaging of cells activated by an experience with tissue-clearing methods or calcium imaging of TRAPed neurons with genetically encoded calcium indicators (Zariwala et al., 2012).

Furthermore, because marker protein expression with TRAP is permanent, analysis of TRAPed cells can be performed long after TRAPing has occurred. This increased temporal flexibility can be utilized to allow the fluorescent marker to diffuse throughout the cell to reveal detailed neuronal morphologies; for instance, long-distance corticothalamic axons from layer 6 neocortical cells were strongly labeled in TRAP mice with the tdTomato reporter (Figure 2). The distribution of synapses made by TRAPed cells can be visualized with synaptically localized fluorescent probes (e.g., Li et al., 2010; see also JAX stock #012570). This temporal flexibility is also advantageous for optogenetics applications, where efficient membrane trafficking and high expression level are critical (Zhang et al., 2010).

Distinguishing between Neurons Activated by Two Experiences

By distinguishing between nuclear and cytoplasmic transcripts of a single IEG or between the transcripts of two IEGs that are produced with different kinetics, compartment analysis of temporal activity by fluorescence in situ hybridization (catFISH) allows cells activated by two temporally separated stimuli to be identified. For catFISH, the two stimuli must be brief (typically ~5 min), and they must be delivered in a restricted time window (typically immediately before and ~30 min before sacrifice; Guzowski et al., 1999). As demonstrated in Figure 5, TRAP can be used to identify populations of cells activated during two

different epochs with fewer temporal constraints than catFISH. With TRAP, cells active during the TRAPing period are genetically marked by the effector, and cells active shortly before the animal is sacrificed are marked by the expression of an IEG. The minimal time between stimulus epochs is only limited by the timecourse of effector expression (e.g., ~3 days for tdTomato; Figure S6), and, because effector expression is permanent, there is no upper limit for the time between epochs. The combination of TRAP and fluorescent reporters of IEG expression (Barth et al., 2004; Kawashima et al., 2009; Wang et al., 2006) will extend the experimental possibilities by allowing cells active during two stimulus epochs to be studied in vivo.

The pioneering TetTag method also allows labeling of populations of cells active during two temporally distant epochs (Reijmers et al., 2007). TetTag utilizes a *Fos*-tTA transgene in which the tetracycline transactivator tTA is driven by a fragment from the *Fos* promoter. A second tTA-dependent transgene expresses a label along with a constitutively active form of tTA (tTA*). Removal of the tTA inhibitor doxycycline opens a time window during which tTA in active cells drives tTA* expression in order to initiate a positive feedback loop that produces permanent expression of tTA*, which is maintained even after the return of doxycycline. Thus, neurons active during the absence of doxycycline will be permanently tagged, whereas neurons active shortly before sacrifice can be identified by IEG immunostaining (Reijmers et al., 2007).

TRAP has several advantages over TetTag. Although the time window for effective tagging with TetTag has not been reported, it is likely to be very long because of the slow timecourse of tTA activation following removal of doxycycline; maximal tTA-dependent gene expression is reached only up to two weeks after stopping Dox administration (Glazewski et al., 2001). In contrast, we show that TRAP can integrate activity over a time window of <12 hr (Figure 4). The transcriptional positive feedback loop that maintains expression of the label with TetTag may also not be fully self-perpetuating, such that tagging with TetTag is not completely permanent. Because recombination is irreversible, labeling with TRAP is permanent. TetTag also suffers from relatively high background levels of tagging, even in mice that are maintained on doxycycline (Liu et al., 2012; Reijmers et al., 2007) and in mice that have only the tTA* and reporter transgenes without the *Fos*-tTA component (K.M., unpublished data). In contrast, FosTRAP produces essentially no recombination in the absence of TM (Figure 2), and background levels of recombination with TM are low in sensory systems that are deprived of input (Figures 2–4).

Manipulating the Activities of Transiently Active Neurons

Expression of optogenetic and pharmacogenetic effectors for reactivation and inhibition of the TRAPed population is an exciting future direction. The Daun02 inactivation method is one alternative approach for inactivating a neuronal population defined by IEG expression (Koya et al., 2009). This method utilizes *Fos-lacZ* rats that are injected with Daun02, a prodrug that is converted by the *lacZ* product to daunorubicin, a putative inhibitor of neuronal activity. Recently active cells that express *lacZ* are thought to be selectively inactivated after converting Daun02 to daunorubicin, although the nature and time course of this inactivation is not well characterized (Koya et al., 2009). Because TRAP can be combined with many well-characterized optogenetic and pharmacogenetic tools, it offers greater flexibility than the Daun02 inactivation method. As an alternative, the *Fos*-tTA component of TetTag has been used to drive the expression of optogenetic and pharmacogenetic tools from viruses (Garner et al., 2012; Liu et al., 2012). This strategy suffers from many of the same limitations as TetTag, including poor temporal resolution and high background. In addition, with the *Fos*-tTA transgene alone, tagging is not permanent; subsequent analysis or manipulation of the tagged population after the return of doxycycline is limited by the perdurance of the effector protein in the absence of active transcription.

Other Genetic Manipulations

Besides the expression of fluorescent labels and of optogenetic and pharmacogenetic tools, additional genetic manipulations of the TRAPed population are also possible. For instance, TRAP can be combined with rabies-virus-based genetically targeted *trans*-synaptic tracing methods in order to identify neurons that connect to TRAPed cells (Miyamichi et al., 2011; Wickersham et al., 2007). By expressing Cre-dependent transgenes (e.g., wild-type genes for gain-of-function experiments or dominant-negative alleles for loss-of-function experiments) or utilizing loxP knockin alleles for Cre-dependent inactivation of a gene, it will also be possible to manipulate genes and proteins in the TRAPed population. These strategies will be useful both for characterizing the roles of the targeted genes and proteins as well as for manipulating the functions of the TRAPed population. The efficiency of Cre recombination is an important consideration for such experiments, given that we have found efficient Cre-dependent transgenes to be critical for successful TRAPing (data not shown). Fortunately, many high-efficiency transgenes identical in locus and design to the AI14 transgene used here have been developed for Cre-dependent expression of fluorescent proteins, optogenetic tools, and calcium indicators (Madisen et al., 2012; Madisen et al., 2010; Zariwala et al., 2012). In addition, advances in site-specific transgenesis techniques now allow the rapid development of additional high-efficiency Cre-dependent transgenes (Tasic et al., 2011). We have also successfully used TRAP in conjunction with viral expression of effector genes (data not shown).

The Nature of the TRAPed Population

An understanding of the features of neuronal activity that lead to IEG expression and TRAPing will be important for applying TRAP. The relationship between synaptic activity and IEG expression is not completely understood and appears to be dependent on many factors. In some cases, spiking alone is sufficient for IEG induction (Schoenenberger et al., 2009), whereas, in other cases, synaptic activation is critical (Luckman et al., 1994). The precise pattern of activity, as well as the duration and intensity of activity, affects IEG induction, and different IEGs have different thresholds of induction (Sheng et al., 1993; Worley et al., 1993). In addition, TRAP is binary (cells are either TRAPed or not), whereas IEG expression is graded (Schoenenberger et al., 2009; Worley et al., 1993). The probability of TRAPing is an unknown function of CreER^{T2} expression level during the critical time window surrounding TM or 4-OHT

injection. Given that the functions relating recombination probability, IEG and CreER^{T2} expression level, and neuronal activity in TRAP are unknown, the electrophysiological responses of the TRAPed population to the experimental stimulus are difficult to predict a priori. On one extreme, the TRAPed population may be a small, stochastic subset of a large population of cells that was weakly activated by the stimulus. On the other extreme, the TRAPed population may be a large percentage of a small population of cells that was strongly activated by the stimulus. Although more effort is necessary to fully distinguish between these possibilities, our observation of good correspondence between TRAPing and Fos expression in the cochlear nucleus (Figure 5) suggests that, at least in this system, the TRAPed population consists mostly of neurons that reliably express Fos at high levels in response to repeated presentation of the same stimulus. Through in vivo targeted electrophysiological and imaging experiments, it will be possible in the future to characterize the physiological responses of a TRAPed population. Such experiments will improve our understanding of how IEG expression is related to cells' physiological properties.

Limitations and Possible Future Improvements of TRAP

The cell-type specificity of TRAP is a limitation for some applications. For instance, we found that, after visual stimulation, GABAergic cells were underrepresented among the TRAPed population (Figure S4). This is consistent with prior work using Fos immunostaining in cats and rats (Mainardi et al., 2009; Van der Gucht et al., 2002). TRAPing of GABAergic cells is likely to be dependent on the stimulus and brain region, and we observed robust TRAPing of some inhibitory neuron types, such as olfactory bulb granule cells and striatal medium spiny neurons (Figure 2). Thus, much of TRAP's cell type specificity is derived from the cell-type specificity of IEG expression. Additional factors, such as the displacement of regulatory elements during gene targeting, cell-type differences in the accessibility of the effector locus for recombination, and cell-type differences in the regulation and trafficking of CreER^{T2} could potentially contribute. Nonetheless, we show that most cell types in the brain can be TRAPed with the current version of the method. Future modifications, such as the development of CreER^{T2} knockin alleles for IEGs that are expressed in different neuronal types and that are sensitive to different features of neuronal activity (Schoenenberger et al., 2009; Worley et al., 1993), could extend the approach to cell types that currently cannot be robustly TRAPed.

Another concern is that our CreER^{T2} knockin alleles are expected to be null for *Fos* and *Arc*. We did not observe any abnormalities in ArcTRAP or FosTRAP mice, and we are not aware of any severe phenotypes in previously generated *Arc* and *Fos* heterozygous knockout mice (Johnson et al., 1992; Paylor et al., 1994; Wang et al., 2006; Wang et al., 1992). However, some subtle phenotypes of *Arc* or *Fos* haploinsufficiency have been reported. These include a low penetrance of increased seizure susceptibility in *Arc*$^{+/-}$ mice (Peebles et al., 2010), and, for *Fos*$^{+/-}$ mice, increased susceptibility to drug-induced neurotoxicity (Deng et al., 1999) and attenuated morphological changes associated with kindling stimuli in an epilepsy model (Watanabe et al., 1996). Although these phenotypes are unlikely to affect many TRAP experiments, alternative knockin or transgenic strategies that do not produce null alleles could mitigate such concerns.

Given that considerable recombination is induced in many brain areas that process sensory information even under homecage conditions, the use of sensory deprivation is useful for improving TRAP specificity (Figure 2). Some noise is likely due to the still relatively long <12 hr period surrounding 4-OHT injection in which any highly active neurons can be TRAPed, regardless of whether or not their activity is related to the experimental stimulus. The use of a destabilized form of CreER^{T2}, the inclusion of endogenous sequences in the *Fos* and *Arc* 3′UTRs that contribute to mRNA destabilization, the development of new CreER ligands that are more rapidly absorbed and metabolized than 4-OHT, and the development of drug-dependent recombinases with reduced leakiness and improved inducibility may result in an improved signal-to-noise ratio. Nonetheless, complex experiences, such as exploration of a novel environment, can increase TRAPing above homecage levels (Figure 6), suggesting that the current version of TRAP has sufficient signal-to-noise ratio without sensory deprivation.

Despite the limitations, we have shown that TRAP provides valuable genetic access to active populations of neurons with feature selectivity in multiple systems. Thus, TRAP can be used in combination with various Cre-dependent effectors to trace connectivity, record activity, and manipulate functions of these select neuronal populations. Although previous methods, such as TetTag, also enabled genetic manipulation of functionally defined neuronal populations, TRAP's superior temporal resolution and its ability to provide permanent genetic access make it a major advancement that has the potential to enable previously impossible experiments.

EXPERIMENTAL PROCEDURES

Methods for mouse production and histology can be found in the Supplemental Experimental Procedures. All mouse procedures were approved by the Stanford University Administrative Panel on Laboratory Animal Care and were in accordance with all applicable regulatory standards. Arc^{CreER} (JAX stock #021881) and Fos^{CreER} (JAX stock #021882) mice can be requested from the Jackson Laboratory.

Tamoxifen Induction

In pilot experiments, we tested a range of TM doses (30–150 mg/kg) and found that TM-induced recombination was highly nonlinear. Low TM doses (30 mg/kg TM) induced minimal recombination, particularly in the less-sensitive FosTRAP mice (data not shown). Given that 150 mg/kg TM induced robust recombination and was well tolerated by the mice, this dose was used for further studies. Similarly, 15 mg/kg 4-OHT induced minimal recombination in FosTRAP mice, whereas 150 mg/kg 4-OHT was not well tolerated. For additional studies, 50 mg/kg was used. In V1 (see Figure 4), treatment with 150 mg/kg TM and 50 mg/kg 4-OHT produced similar total numbers of TRAPed cells both in the dark condition (4-OHT, 622 ± 110 cells/mm^3; TM, 777 ± 191 cells/mm^3; t[7] = 0.65, p = 0.53) and when administered at the time point for optimal TRAPing (0 hr 4-OHT, 5184 ± 605 cells/mm^3; 24 hr TM, 5736 ± 731 cells/mm^3; t[9] = 0.57, p = 0.59). We also found that 4-OHT produced more consistent results than TM. In 5%–20% of mice treated with TM, induction appeared to fail altogether, and so few cells were labeled that the mice were excluded from analysis. Similar failures were never observed in mice treated with 4-OHT. For details of TM and 4-OHT preparation, see the Supplemental Experimental Procedures.

Stimulation Conditions

For barrel cortex experiments, mice were anesthetized with 100 mg/kg ketamine and 10 mg/kg xylazine i.p. injected, and whiskers were removed under a dissection scope by grasping them at the base with forceps and pulling. After whisker removal, mice were singly housed, and whiskers did not regrow substantially by the time of tamoxifen injection two days later. Approximately 6 hr after TM injection, mice were provided with cardboard tubes (approximately 3.5 cm in diameter) and nesting material to stimulate whisker exploration.

For visual stimulation, the homecages of singly housed mice were placed in individual light-tight cubicles with white walls. Light stimuli were delivered by an LED bulb mounted above the cage, which produced light of ~500 lux at cage level. Drugs were injected with a dim red LED in an otherwise dark room. For the time course experiment, light was delivered at the same time of day (starting at 8 hr after the subjective dawn of the animal's former light/dark cycle) to all mice in order to control for possible circadian differences in sensitivity to stimulation, and the timing of drug injections was varied around this fixed time.

For auditory stimulation, mice were placed into custom sound isolation cubicles lined with acoustic foam (Auralex Acoustics). Sound stimuli were generated in Audacity (https://audacity.sourceforge.net), produced by a PC sound card (Creative Labs), amplified (Onkyo), and delivered by a speaker (Fostex) mounted directly above the animal's cage. Stimuli were delivered at approximately 90 dB.

For the novel environment experiments, mice were group housed until at least 3 days before the start of the experiment, at which point they were singly housed in standard 20 × 30 cm mouse cages in a normal colony room. Novel environment experiments were performed beginning 1–3 hr after the onset of the animals' dark cycle, at which point experimental mice were transported to a separate room and placed in a dimly lit (<10 lux) 30 × 60 cm plastic cage with a running wheel, a wooden or plastic "hut," a plastic tunnel, wooden chips for chewing, and buried food. After 1 hr, mice were removed from the novel environment and injected with either 4-OHT or vehicle before they were returned to the novel environment for another 1 hr, at which point they were returned to the homecage in the animal colony for 1 week before sacrifice. Homecage control mice were similarly injected with 4-OHT 1–3 hr after the onset of the dark cycle under dim white light 1 week prior to sacrifice.

For all experiments, mice were subjected to only the minimal handling necessary for genotyping and colony maintenance prior to performing the experiments.

Data Analysis

Details of cell counting and quantification are available in the Supplemental Experimental Procedures. Statistical analyses were performed in Prism (GraphPad).

SUPPLEMENTAL INFORMATION

Supplemental Information contains Supplemental Experimental Procedures and six figures and can be found with this article online at http://dx.doi.org/10.1016/j.neuron.2013.03.025.

ACKNOWLEDGMENTS

We thank A. Huberman, A. Mizrahi, and C. Ran for advice; members of the Heller lab for help with preliminary experiments; B. Tasic for DNA constructs and advice; C. Manalac and K. DeLoach for technical assistance; the Stanford Transgenic Facility for help in generating mice; K. Beier, K. Deisseroth, L. DeNardo, X. Gao, C. Golgi, A. Huberman, N. Makki, A. Mizrahi, T. Mosca, L. Schwarz, and B. Weissbourd for helpful comments on the manuscript; and members of the Luo lab for helpful discussion. This work was supported by grants from the National Institutes of Health (NIH; R01-NS050835 and TR01MH099647), the Simons Foundation, and by a Howard Hughes Medical Institute (HHMI) Collaborative Innovation Award. C.J.G. is supported by the U.S. Department of Defense through the National Defense Science and Engineering Graduate Fellowship program. H.H.Y. is a Stanford Graduate Fellow. K.M. was supported by the Human Frontier Science Program Organization (LT00300/2007-L). K.M. is a research specialist and L.L. is an investigator of the HHMI.

Accepted: March 19, 2013
Published: June 5, 2013

REFERENCES

Amir, S., and Robinson, B. (1996). Fos expression in rat visual cortex induced by ocular input of ultraviolet light. Brain Res. *716*, 213–218.

Armstrong-James, M., Fox, K., and Das-Gupta, A. (1992). Flow of excitation within rat barrel cortex on striking a single vibrissa. J. Neurophysiol. *68*, 1345–1358.

Barth, A.L., Gerkin, R.C., and Dean, K.L. (2004). Alteration of neuronal firing properties after in vivo experience in a FosGFP transgenic mouse. J. Neurosci. *24*, 6466–6475.

Chawla, M.K., Guzowski, J.F., Ramirez-Amaya, V., Lipa, P., Hoffman, K.L., Marriott, L.K., Worley, P.F., McNaughton, B.L., and Barnes, C.A. (2005). Sparse, environmentally selective expression of Arc RNA in the upper blade of the rodent fascia dentata by brief spatial experience. Hippocampus *15*, 579–586.

Deng, X., Ladenheim, B., Tsao, L.-I., and Cadet, J.L. (1999). Null mutation of c-fos causes exacerbation of methamphetamine-induced neurotoxicity. J. Neurosci. *19*, 10107–10115.

Feil, R., Wagner, J., Metzger, D., and Chambon, P. (1997). Regulation of Cre recombinase activity by mutated estrogen receptor ligand-binding domains. Biochem. Biophys. Res. Commun. *237*, 752–757.

Friauf, E. (1992). Tonotopic order in the adult and developing auditory system of the rat as shown by c-fos immunocytochemistry. Eur. J. Neurosci. *4*, 798–812.

Garner, A.R., Rowland, D.C., Hwang, S.Y., Baumgaertel, K., Roth, B.L., Kentros, C., and Mayford, M. (2012). Generation of a synthetic memory trace. Science *335*, 1513–1516.

Glazewski, S., Bejar, R., Mayford, M., and Fox, K. (2001). The effect of autonomous alpha-CaMKII expression on sensory responses and experience-dependent plasticity in mouse barrel cortex. Neuropharmacology *41*, 771–778.

Guzowski, J.F., McNaughton, B.L., Barnes, C.A., and Worley, P.F. (1999). Environment-specific expression of the immediate-early gene Arc in hippocampal neuronal ensembles. Nat. Neurosci. *2*, 1120–1124.

Hess, U.S., Lynch, G., and Gall, C.M. (1995). Regional patterns of c-fos mRNA expression in rat hippocampus following exploration of a novel environment versus performance of a well-learned discrimination. J. Neurosci. *15*, 7796–7809.

Johnson, R.S., Spiegelman, B.M., and Papaioannou, V. (1992). Pleiotropic effects of a null mutation in the c-fos proto-oncogene. Cell *71*, 577–586.

Kaczmarek, L., and Chaudhuri, A. (1997). Sensory regulation of immediate-early gene expression in mammalian visual cortex: implications for functional mapping and neural plasticity. Brain Res. Brain Res. Rev. *23*, 237–256.

Kawashima, T., Okuno, H., Nonaka, M., Adachi-Morishima, A., Kyo, N., Okamura, M., Takemoto-Kimura, S., Worley, P.F., and Bito, H. (2009). Synaptic activity-responsive element in the Arc/Arg3.1 promoter essential for synapse-to-nucleus signaling in activated neurons. Proc. Natl. Acad. Sci. USA *106*, 316–321.

Koya, E., Golden, S.A., Harvey, B.K., Guez-Barber, D.H., Berkow, A., Simmons, D.E., Bossert, J.M., Nair, S.G., Uejima, J.L., Marin, M.T., et al. (2009). Targeted disruption of cocaine-activated nucleus accumbens neurons prevents context-specific sensitization. Nat. Neurosci. *12*, 1069–1073.

Li, L., Tasic, B., Micheva, K.D., Ivanov, V.M., Spletter, M.L., Smith, S.J., and Luo, L. (2010). Visualizing the distribution of synapses from individual neurons in the mouse brain. PLoS ONE *5*, e11503.

Lin, D., Boyle, M.P., Dollar, P., Lee, H., Lein, E.S., Perona, P., and Anderson, D.J. (2011). Functional identification of an aggression locus in the mouse hypothalamus. Nature *470*, 221–226.

Liu, X., Ramirez, S., Pang, P.T., Puryear, C.B., Govindarajan, A., Deisseroth, K., and Tonegawa, S. (2012). Optogenetic stimulation of a hippocampal engram activates fear memory recall. Nature *484*, 381–385.

Luckman, S.M., Dyball, R.E., and Leng, G. (1994). Induction of c-fos expression in hypothalamic magnocellular neurons requires synaptic activation and not simply increased spike activity. J. Neurosci. *14*, 4825–4830.

Luo, L., Callaway, E.M., and Svoboda, K. (2008). Genetic Dissection of Neural Circuits. Neuron *57*, 634–660.

Luo, F., Wang, Q., Farid, N., Liu, X., and Yan, J. (2009). Three-dimensional tonotopic organization of the C57 mouse cochlear nucleus. Hear. Res. *257*, 75–82.

Lyford, G.L., Yamagata, K., Kaufmann, W.E., Barnes, C.A., Sanders, L.K., Copeland, N.G., Gilbert, D.J., Jenkins, N.A., Lanahan, A.A., and Worley, P.F. (1995). Arc, a growth factor and activity-regulated gene, encodes a novel cytoskeleton-associated protein that is enriched in neuronal dendrites. Neuron *14*, 433–445.

Madisen, L., Zwingman, T.A., Sunkin, S.M., Oh, S.W., Zariwala, H.A., Gu, H., Ng, L.L., Palmiter, R.D., Hawrylycz, M.J., Jones, A.R., et al. (2010). A robust and high-throughput Cre reporting and characterization system for the whole mouse brain. Nat. Neurosci. *13*, 133–140.

Madisen, L., Mao, T., Koch, H., Zhuo, J.M., Berenyi, A., Fujisawa, S., Hsu, Y.-W.A., Garcia, A.J., 3rd, Gu, X., Zanella, S., et al. (2012). A toolbox of Cre-dependent optogenetic transgenic mice for light-induced activation and silencing. Nat. Neurosci. *15*, 793–802.

Mainardi, M., Landi, S., Berardi, N., Maffei, L., and Pizzorusso, T. (2009). Reduced responsiveness to long-term monocular deprivation of parvalbumin neurons assessed by c-Fos staining in rat visual cortex. PLoS ONE *4*, e4342.

Miyamichi, K., Amat, F., Moussavi, F., Wang, C., Wickersham, I., Wall, N.R., Taniguchi, H., Tasic, B., Huang, Z.J., He, Z., et al. (2011). Cortical representations of olfactory input by trans-synaptic tracing. Nature *472*, 191–196.

Morgan, J.I., Cohen, D.R., Hempstead, J.L., and Curran, T. (1987). Mapping patterns of c-fos expression in the central nervous system after seizure. Science *237*, 192–197.

Ohki, K., Chung, S., Ch'ng, Y.H., Kara, P., and Reid, R.C. (2005). Functional imaging with cellular resolution reveals precise micro-architecture in visual cortex. Nature *433*, 597–603.

Paylor, R., Johnson, R.S., Papaioannou, V., Spiegelman, B.M., and Wehner, J.M. (1994). Behavioral assessment of c-fos mutant mice. Brain Res. *651*, 275–282.

Peebles, C.L., Yoo, J., Thwin, M.T., Palop, J.J., Noebels, J.L., and Finkbeiner, S. (2010). Arc regulates spine morphology and maintains network stability in vivo. Proc. Natl. Acad. Sci. USA *107*, 18173–18178.

Petersen, C.C.H. (2007). The functional organization of the barrel cortex. Neuron *56*, 339–355.

Reijmers, L.G., Perkins, B.L., Matsuo, N., and Mayford, M. (2007). Localization of a stable neural correlate of associative memory. Science *317*, 1230–1233.

Robinson, S.P., Langan-Fahey, S.M., Johnson, D.A., and Jordan, V.C. (1991). Metabolites, pharmacodynamics, and pharmacokinetics of tamoxifen in rats and mice compared to the breast cancer patient. Drug Metab. Dispos. *19*, 36–43.

Rothschild, G., Nelken, I., and Mizrahi, A. (2010). Functional organization and population dynamics in the mouse primary auditory cortex. Nat. Neurosci. *13*, 353–360.

Saint Marie, R.L., Luo, L., and Ryan, A.F. (1999). Effects of stimulus frequency and intensity on c-fos mRNA expression in the adult rat auditory brainstem. J. Comp. Neurol. *404*, 258–270.

Schoenenberger, P., Gerosa, D., and Oertner, T.G. (2009). Temporal control of immediate early gene induction by light. PLoS ONE *4*, e8185.

Sheng, M., and Greenberg, M.E. (1990). The regulation and function of c-fos and other immediate early genes in the nervous system. Neuron *4*, 477–485.

Sheng, H.Z., Fields, R.D., and Nelson, P.G. (1993). Specific regulation of immediate early genes by patterned neuronal activity. J. Neurosci. Res. *35*, 459–467.

Smeyne, R.J., Schilling, K., Robertson, L., Luk, D., Oberdick, J., Curran, T., and Morgan, J.I. (1992). fos-lacZ transgenic mice: mapping sites of gene induction in the central nervous system. Neuron *8*, 13–23.

Staiger, J.F., Bisler, S., Schleicher, A., Gass, P., Stehle, J.H., and Zilles, K. (2000). Exploration of a novel environment leads to the expression of inducible transcription factors in barrel-related columns. Neuroscience *99*, 7–16.

Stettler, D.D., and Axel, R. (2009). Representations of odor in the piriform cortex. Neuron *63*, 854–864.

Tasic, B., Hippenmeyer, S., Wang, C., Gamboa, M., Zong, H., Chen-Tsai, Y., and Luo, L. (2011). Site-specific integrase-mediated transgenesis in mice via pronuclear injection. Proc. Natl. Acad. Sci. USA *108*, 7902–7907.

Van der Gucht, E., Clerens, S., Cromphout, K., Vandesande, F., and Arckens, L. (2002). Differential expression of c-fos in subtypes of GABAergic cells following sensory stimulation in the cat primary visual cortex. Eur. J. Neurosci. *16*, 1620–1626.

Wang, Z.-Q., Ovitt, C., Grigoriadis, A.E., Möhle-Steinlein, U., Rüther, U., and Wagner, E.F. (1992). Bone and haematopoietic defects in mice lacking c-fos. Nature *360*, 741–745.

Wang, K.H., Majewska, A., Schummers, J., Farley, B., Hu, C., Sur, M., and Tonegawa, S. (2006). In vivo two-photon imaging reveals a role of arc in enhancing orientation specificity in visual cortex. Cell *126*, 389–402.

Watanabe, Y., Johnson, R.S., Butler, L.S., Binder, D.K., Spiegelman, B.M., Papaioannou, V.E., and McNamara, J.O. (1996). Null mutation of c-fos impairs structural and functional plasticities in the kindling model of epilepsy. J. Neurosci. *16*, 3827–3836.

Wickersham, I.R., Lyon, D.C., Barnard, R.J.O., Mori, T., Finke, S., Conzelmann, K.-K., Young, J.A.T., and Callaway, E.M. (2007). Monosynaptic restriction of transsynaptic tracing from single, genetically targeted neurons. Neuron *53*, 639–647.

Worley, P.F., Bhat, R.V., Baraban, J.M., Erickson, C.A., McNaughton, B.L., and Barnes, C.A. (1993). Thresholds for synaptic activation of transcription factors in hippocampus: correlation with long-term enhancement. J. Neurosci. *13*, 4776–4786.

Young, E.D., and Oertel, D. (2004). Cochlear nucleus. In The synaptic organization of the brain, G.M. Shepard, ed. (New York, NY: Oxford University Press).

Zariwala, H.A., Borghuis, B.G., Hoogland, T.M., Madisen, L., Tian, L., De Zeeuw, C.I., Zeng, H., Looger, L.L., Svoboda, K., and Chen, T.-W. (2012). A Cre-dependent GCaMP3 reporter mouse for neuronal imaging in vivo. J. Neurosci. *32*, 3131–3141.

Zhang, F., Gradinaru, V., Adamantidis, A.R., Durand, R., Airan, R.D., de Lecea, L., and Deisseroth, K. (2010). Optogenetic interrogation of neural circuits: technology for probing mammalian brain structures. Nat. Protoc. *5*, 439–456.

Neuron, Volume *78*
Supplemental Information

Permanent Genetic Access to Transiently Active Neurons via TRAP: Targeted Recombination in Active Populations

Casey J. Guenthner, Kazunari Miyamichi, Helen H. Yang, H. Craig Heller, and Liqun Luo

Inventory of Supplemental Information

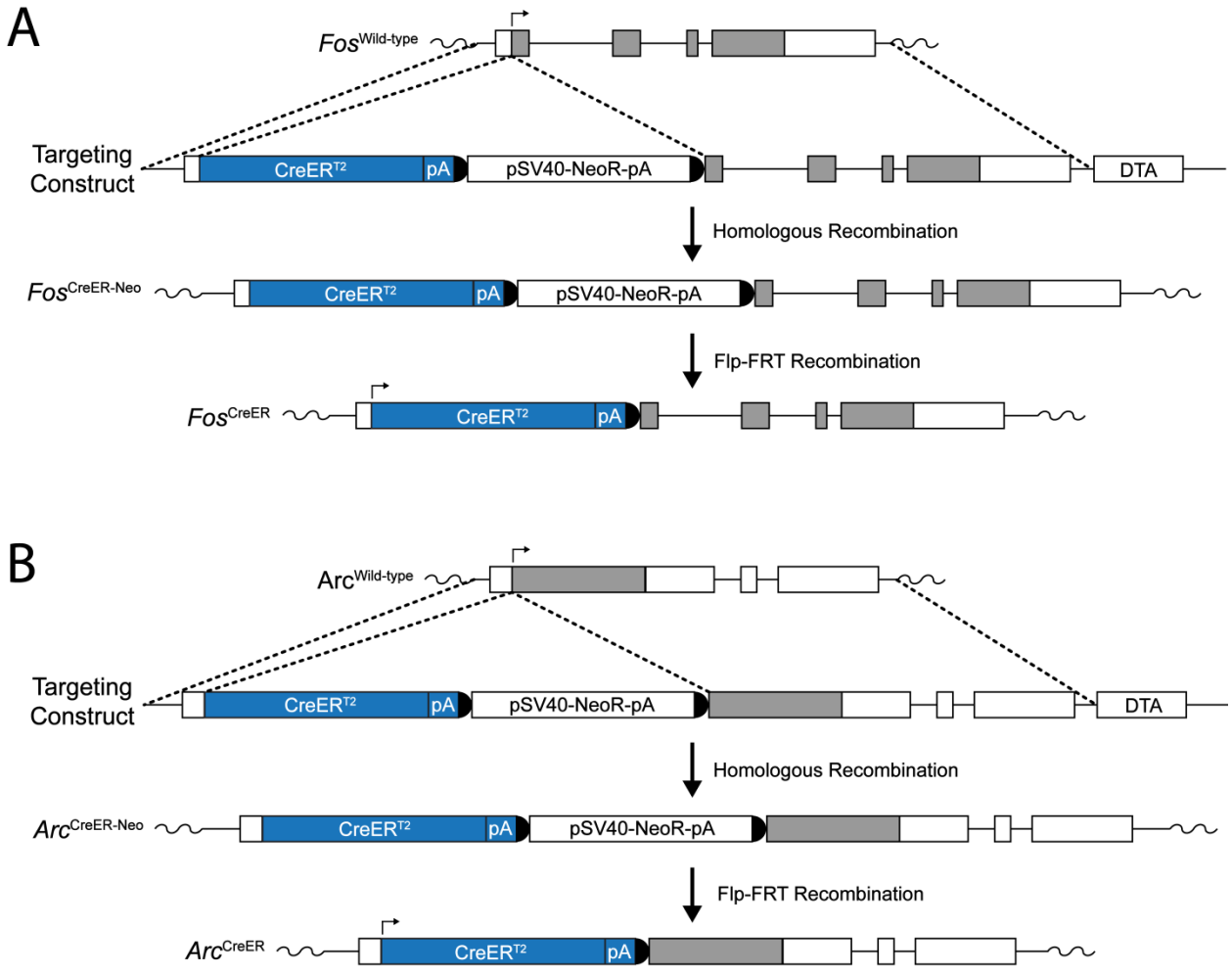

Figure S1. Detailed Gene Targeting Scheme for the Production of *Arc*^{CreER} and *Fos*^{CreER} Knockin Alleles, Related to Figure 1

Open rectangles indicate exons, and protein-coding regions are indicated with grey shading. The CreER^{T2}-SV40 polyA cassette is indicated in blue. Black half-circles symbolize the FRT5 flanking the neomycin resistance gene driven by the SV40 promoter (pSV40-NeoR-pA cassette), which was used for positive selection. DTA indicates the diphtheria toxin A cassette used for negative selection. Wavy lines represent adjacent genomic DNA. Flp-FRT recombination was performed *in vivo* by crossing the targeted allele to a germline-active FlpO line.

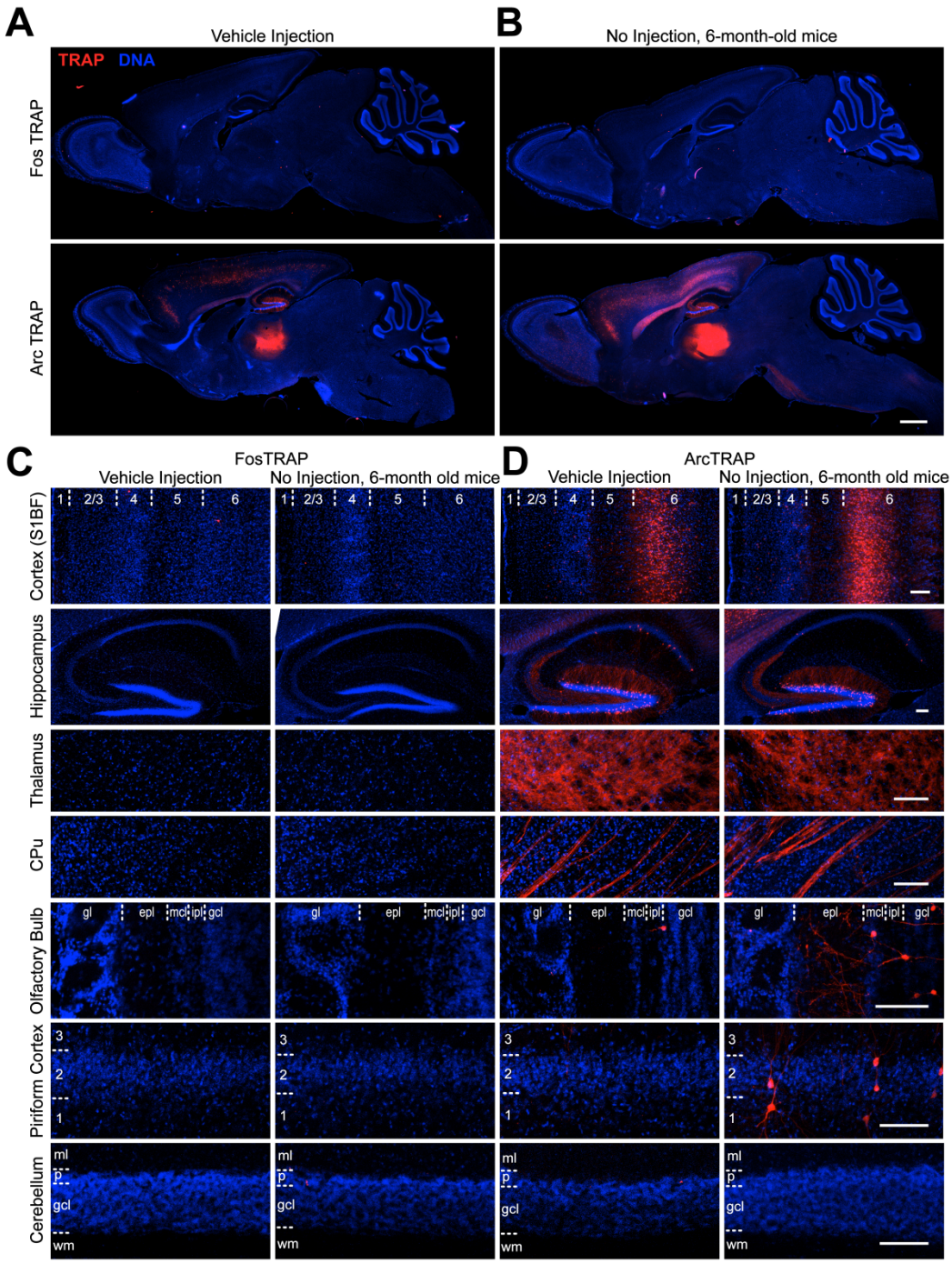

Figure S2. Effects of Vehicle Injection and Aging on TRAPing, Related to Figure 2

(A and B) Full sagittal views of FosTRAP (top) and ArcTRAP (bottom) brains from 6-8 week old mice injected with tamoxifen vehicle (A) or from 6-month-old mice that were untreated (B). Scale bar, 1 mm.
(C and D) Magnified views from 6-8-week-old vehicle-treated (left columns) or 6-month-old untreated (right columns) FosTRAP (C) and ArcTRAP (D) brains. Images are representative of at least n=2-3 mice examined per condition and are analogous to those in Figure 2. Scale bar,

100 μm.

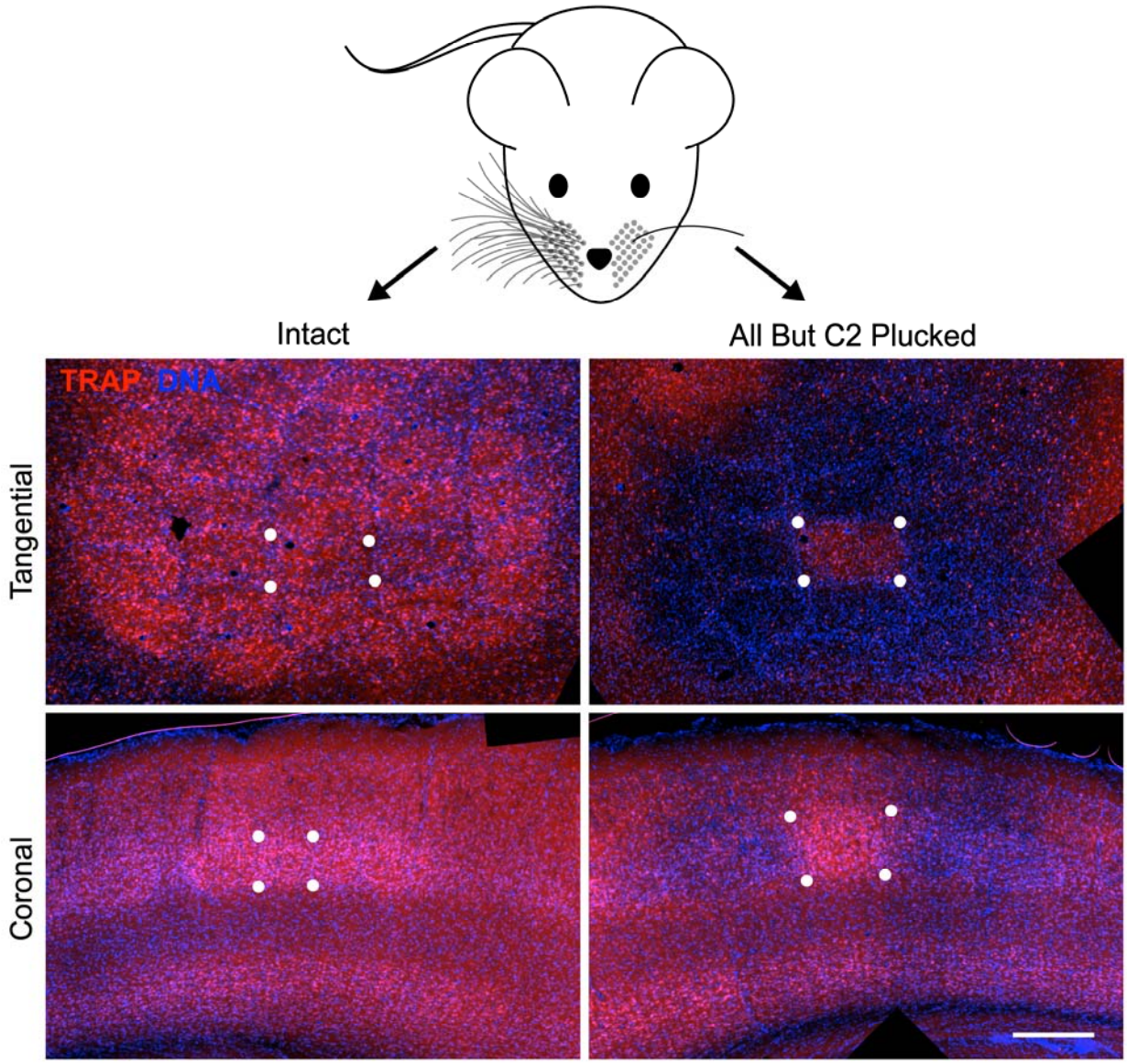

Figure S3. ArcTRAP in the Barrel Cortex of Whisker-Plucked Mice, Related to Figure 3

ArcTRAP mice had all whiskers except C2 plucked on one side and two days later were injected with 150 mg/kg TM. 7 days after injection, they were sacrificed. In barrel cortex contralateral to the intact side (left), TRAPed cells are distributed evenly across barrels (left). However, in barrel cortex contralateral to the plucked side, only the C2 barrel is labeled (right). Scale bar, 250 μm.

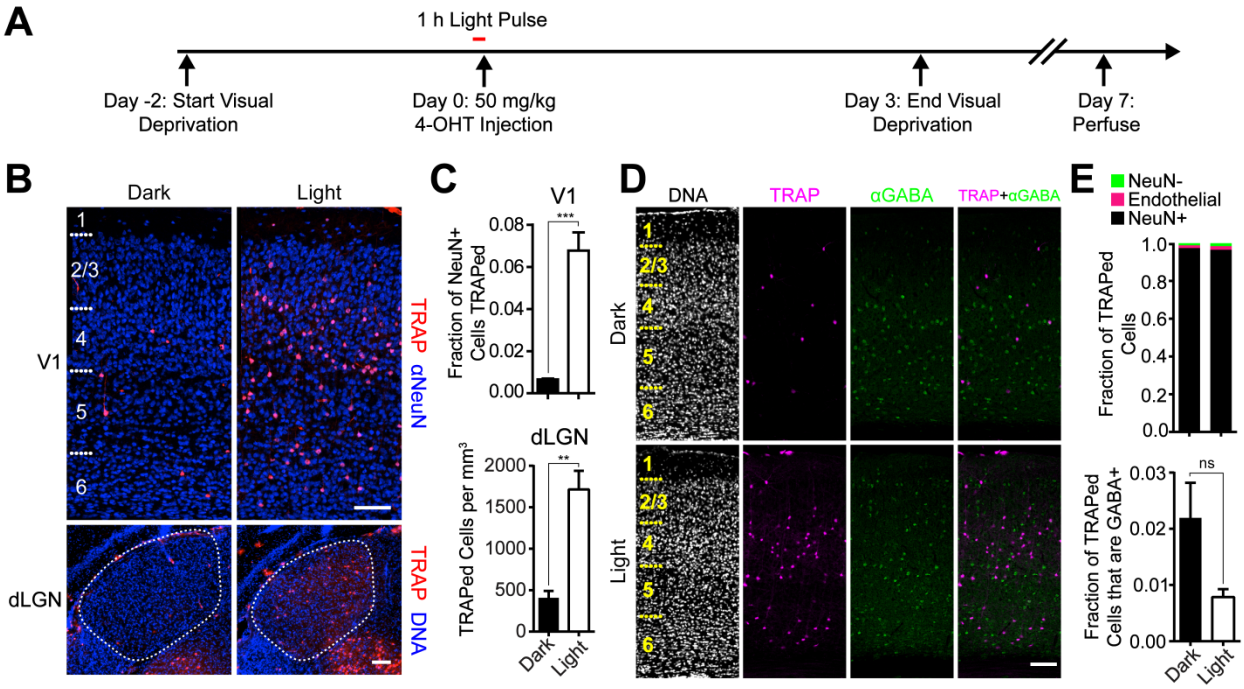

Figure S4. Additional Data of FosTRAP in the Visual System, Related to Figure 4

(A) Experimental scheme: FosTRAP mice were placed in constant darkness for five days (from day -2 to day 3). Light-treated mice were given a 1 h light pulse before a 50 mg/kg 4-OHT injection on day 0. Mice were perfused 7 days after injection.
(B) Images of primary visual cortex (top) and the dorsal lateral geniculate nucleus (dLGN, outlined in the bottom panels) from mice that were left in the dark (left) or that were exposed to light before 4-OHT injection. Light induced TRAPing of cells in both V1 and the dLGN.
(C) Quantification of the fraction of TRAPed NeuN+ neurons in V1 (top) and of the density of TRAPed cells in the dLGN (bottom; mean ± SEM, n = 4 mice per condition). A significantly larger fraction of neurons in V1 was TRAPed in light-stimulated mice than in dark control mice (two-tailed t test, $p<0.001$), and light stimulation also increased the density of TRAPed cells in the dLGN (two-tailed t test, $p<0.01$).
(D) Representative images of visual cortex from light-stimulated (bottom) and dark control (top) mice that were stained for GABA. Few TRAPed cells (magenta) were GABAergic (green) across several sections from each of the 4 mice per condition examined. Scale bars, 100 μm.
(E) Fractions of TRAPed cells that are immunopositive for NeuN (NeuN+, black), that are NeuN- and that have morphologies consistent with endothelial cells (magenta), or that are non-endothelial NeuN- cells (most with morphologies consistent with astrocytes; green; top). Data were pooled across mice (n=50-350 cells per mouse, n=4 mice per condition). Quantification (mean ± SEM, n = 4 mice per condition) of the fraction of all TRAPed cells that are immunopositive for GABA (bottom; ns, difference not statistically significant).

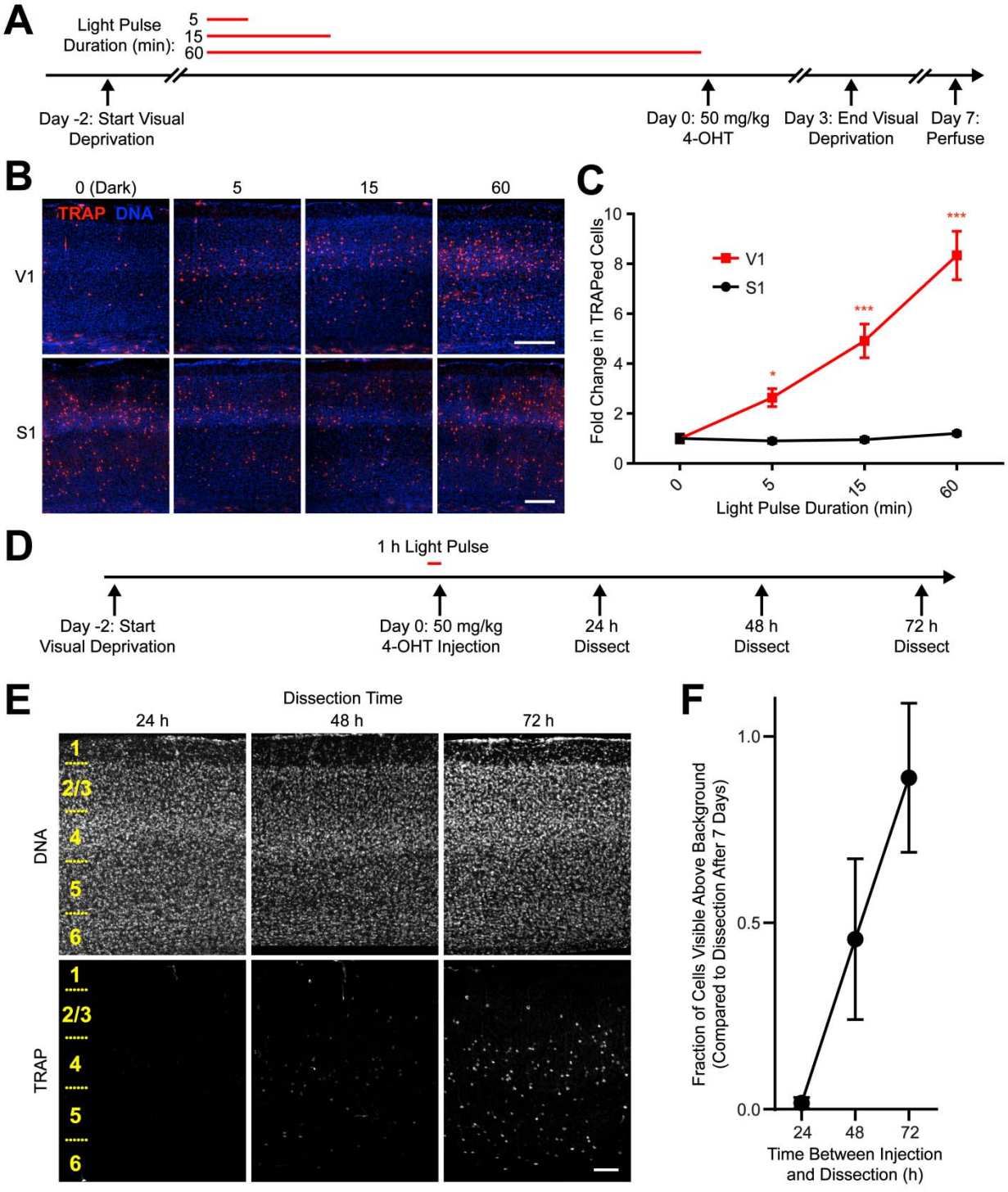
A
Light Pulse Duration (min):
5
15
60
Day -2: Start Visual Deprivation
Day 0: 50 mg/kg 4-OHT
Day 3: End Visual Deprivation
Day 7: Perfuse
B
0 (Dark)
5
15
60
TRAP DNA
V1
S1
C
Fold Change in TRAPed Cells
V1
S1
Light Pulse Duration (min)
D
1 h Light Pulse
Day -2: Start Visual Deprivation
Day 0: 50 mg/kg 4-OHT Injection
24 h Dissect
48 h Dissect
72 h Dissect
E
Dissection Time
24 h
48 h
72 h
DNA
TRAP
1
2/3
4
5
6
F
Fraction of Cells Visible Above Background (Compared to Dissection After 7 Days)
Time Between Injection and Dissection (h)

Figure S5. Effect of Stimulus Duration on TRAPing and the Time Course of tdTomato Expression after TRAPing, Related to Figure 4

(A) Experimental scheme for testing the effect of stimulus duration on TRAP efficiency. FosTRAP mice were placed in constant darkness for 2 days and were then given light pulses 5, 15, or 60 min in duration or were left in the dark (0 min duration light pulse). All mice were injected with 50 mg/kg 4-OHT 60 min after the onset of the light pulse. Mice remained in darkness for three days following drug injection and were sacrificed seven days later.
(B) Representative images of primary visual (V1; top row) and somatosensory (S1; bottom row) cortices from mice exposed to light stimuli of different durations, indicated at the top of each column. The panels for the 0 min (Dark) and 60 min conditions are reproduced from Figure 4. Scale bar, 250 μm.
(C) Quantification (mean ± SEM, n=4-5 mice per time point) of the density of TRAPed cells in V1 and S1, normalized to the mean density of TRAPed cells in the dark (0 min light pulse) condition. Light stimulation did not increase the number of TRAPed cells in S1, regardless of duration, while the number of TRAPed cells in V1 increased with increasing stimulus duration (Holm-Sidak's multiple comparison tests following significant two-way ANOVA with region and stimulus duration as factors: none of the comparisons between stimulus durations were significant for S1, while all comparisons between stimulus durations were significant for V1). * and ***, significantly different from the dark (0 min duration) condition for V1 (*, $p<0.05$; ***, $p<0.001$).
(D) Schematic of the experimental time course to examine the time course of tdTomato expression after TRAPing. Mice were placed in the dark for 2 days and were then given a 1 h light pulse followed by a 50 mg/kg 4-OHT injection. Mice were dissected 24 h, 48 h, or 72 h after injection.
(E) Representative images from n=4 mice per time point. Virtually no tdTomato expression was visible 24 h after light stimulation and injection. Clear tdTomato expression was present at 48 h but increased considerably over the next 24 h. TRAPed cells could reliably be identified in all animals dissected 72 h after injection. Scale bar, 100 μm.
(F) Quantification (mean± SEM, n=4 mice/time point) of the fraction of cells visible above background tissue fluorescence, obtained by dividing the number of cells visible at each dissection time point by the number visible when the animals were dissected after 7 days (which is assumed to represent the total TRAPed population).

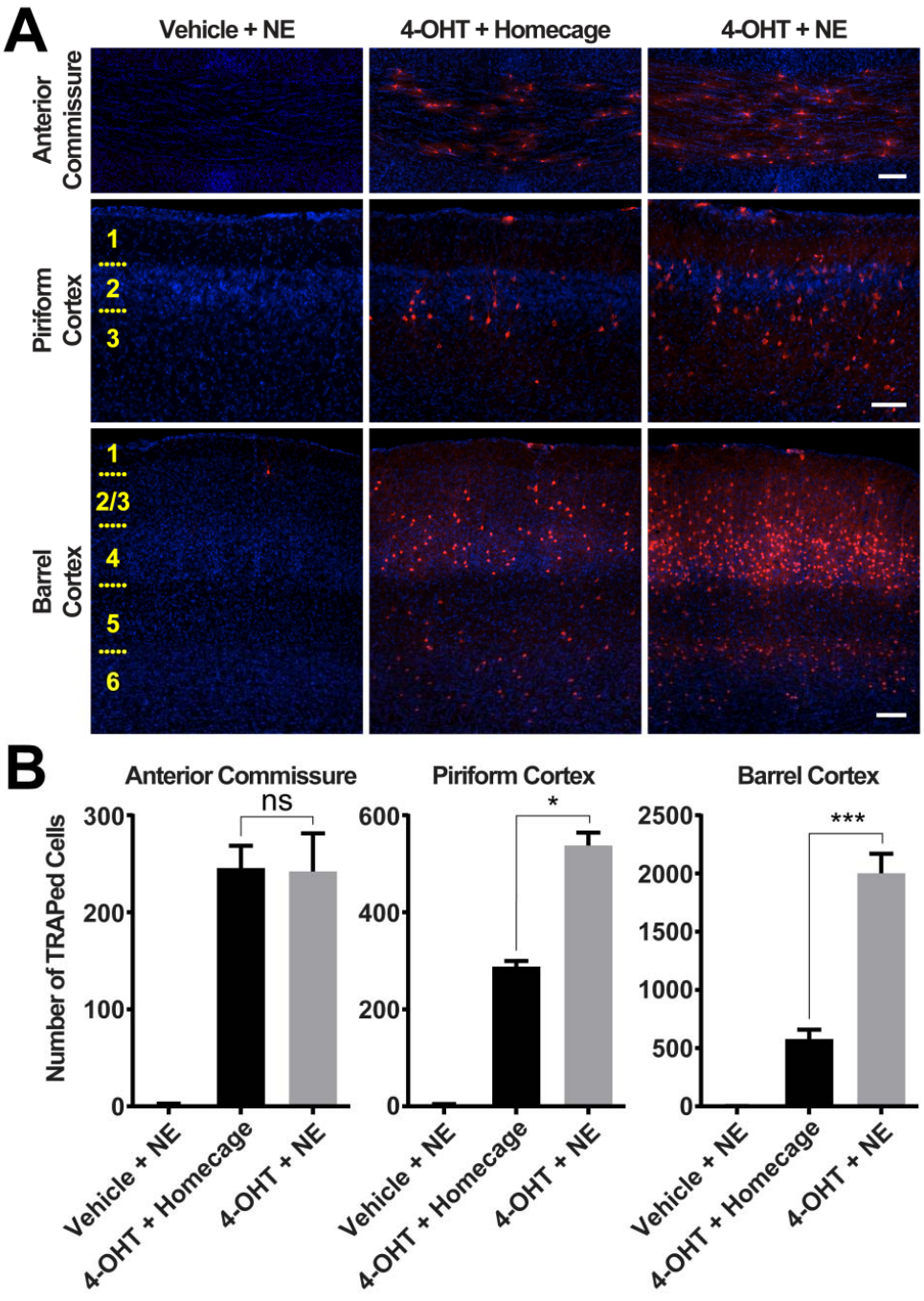
A
Vehicle + NE
4-OHT + Homecage
4-OHT + NE
Anterior Commissure
Piriform Cortex
1
2
3
Barrel Cortex
1
2/3
4
5
6
B
Anterior Commissure
Piriform Cortex
Barrel Cortex
Number of TRAPed Cells
ns
*
***
300
200
100
0
600
400
200
0
2500
2000
1500
1000
500
0
Vehicle + NE
4-OHT + Homecage
4-OHT + NE

Figure S6. Novel Environment Exploration Induces TRAPing in Multiple Brain Areas, Related to Figure 6

(A) Representative images of the anterior commissure (top), the piriform cortex (middle), and the primary somatosensory barrel field (bottom) in mice that received a vehicle injection while exploring a novel environment (left), that received an injection of 50 mg/kg 4-OHT in the homecage (center), and that received a 50 mg/kg 4-OHT injection while exploring a novel environment (right). NE, novel environment. Scale bars, 100 μm.
(B) Quantifiction (mean±SEM, n=6 mice for the two 4-OHT groups and n=3 mice for the vehicle group) of numbers of TRAPed cells in consistent subregions of the anterior commissure (left), the piriform cortex (center), and the primary somatosensory barrel field (right) of mice that were treated with vehicle while exploring a novel environment or that were injected with 4-OHT while in the homecage or while exploring a novel environment. Novel environment exposure increased the numbers of TRAPed cells in the piriform cortex and in barrel cortex but not in the anterior commissure of 4-OHT-treated mice (*, $p<0.05$; ***, $p<0.001$).

SUPPLEMENTAL EXPERIMENTAL PROCEDURES

Mouse Genetics

Targeting constructs for *Arc*^{CreER} and *Fos*^{CreER} alleles were produced using conventional cloning approaches with CreERT2-SV40pA (Feil et al., 1997) and FRT5-pSV40-Neo-pA-FRT5 cassettes (Tasic et al., 2011) and homology arms amplified by high-fidelity PCR (Phusion, Finnzyems) from 129X1/SvJ genomic DNA (Jackson Labs). Since we were initially concerned that CreER^{T2} expression levels would be too low for efficient recombination, our targeting strategy displaced the introns, coding sequences, and endogenous *Fos* and *Arc* 3'UTRs, which are known to contain elements important for mRNA degradation and dendritic localization (Giorgi et al., 2007; Kobayashi et al., 2005; Wilson and Treisman, 1988), to the 3' end of the CreER-SV40pA cassette. After verification by sequencing, the constructs were electroporated into R1 129Sv/SvJ ES cells, and correctly targeted clones were identified by long-range PCR (LA Taq, TaKaRa) and sequencing. Targeted ES cells were microinjected into BL/6 blastocysts, and chimeras were mated to a germline-active GFP-FlpO transgenic line (Tasic et al., 2011) to remove the neomycin resistance cassette. Pups lacking the Neo cassette were identified by PCR and were used to expand the colony. AI14 mice (Madisen et al., 2010) were obtained from Jackson Labs (stock #007914). The *Arc*$^{CreER/+}$ and *Fos*$^{CreER/+}$ mice were crossed to *R26*$^{AI14/+}$ mice to obtain the double heterozygous mice used in these experiments. Homozygous *Arc*$^{CreER/CreER}$ mice are viable and breed normally; we have not attempted to generate *Fos*$^{CreER/CreER}$ mice. Genotyping for AI14 was performed using the standard PCR protocol provided by Jackson Labs. Genotyping for the IEG-CreER alleles was performed using generic Cre primers that produce a ~300 bp band (5'-CACCCTGTTACGTATAGCCG-3'and 5'-GAGTCATCCTTAGCGCCGTA-3') and *Beta-s* primers that produce ~500 bp band as an internal control (5'-CCAATCTGCTCACACAGGATAGAGAGGGCAGG-3' and 5'-CCTTGAGGCTGTCCAAGTGATTCAGGCCATCG-3'). For distinguishing heterozygous *Arc*$^{CreER/+}$ and homozygous *Arc*$^{CreER/CreER}$ mice, the following locus-specific primers may also be used: 5'-GGTGGCGGTTTCGGTGCAGA-3' (common forward), 5'-GCATCGACCGGTAATGCAGGC-3' (CreER reverse), and 5'-TCCAGCTTGCCCACCGACCT-3' (Arc wild-type reverse); the CreER and wild-type alleles give 266 bp and 428 bp bands, respectively. All mice used in these experiments were on heterogeneous mixed genetic backgrounds that included FVB, C57BL/6J, 129Sv, 129SvJ, and/or CD-1. We have not observed any qualitative differences using TRAP mice that have been backcrossed >5 generations onto a C57BL/6J background.

Drug Preparation

Tamoxifen (Sigma, Cat #T5648) was dissolved at 20 mg/mL in corn oil (Sigma, Cat #C8267) by nutation at room temperature for 4-8 h. 4-hydroxytamoxifen (Sigma, Cat# H6278) was dissolved at 20 mg/mL in ethanol by shaking at 37 °C for 15 min and was then aliquoted and stored at -20 °C for up to several weeks. Before use, 4-OHT was redissolved in ethanol by shaking at 37 °C for 15 min, corn oil or Chen Oil [a 1:4 mixture of castor oil:sunflower seed oil (Sigma, Cat #s 259853 and S5007)] was added to give a final concentration of 10 mg/mL 4-OHT, and the ethanol was evaporated by vacuum under centrifugation. The final 20 mg/mL tamoxifen and 10 mg/mL 4-OHT solutions were stored for at most 24 h at 4 °C before use. All injections were delivered intraperitoneally (i.p.).

Histology

Mice were given an overdose of 2.5% Avertin and were perfused transcardially with phosphate buffered saline, pH 7.4 (PBS) followed by 4% paraformaldehyde (PFA) in PBS. Brains were dissected and post-fixed for 16-24 h in 4% PFA in PBS and were cryoprotected for 24-48 h in 30% sucrose.

Flattened cortical sections were prepared as previously described (Strominger and Woolsey, 1987). After perfusion with 4% PFA, brains were post-fixed in 4% PFA in PBS for 2-6 h. Brains were transferred to PBS, and cortex was dissected away from the underlying structures using forceps and micro scissors. The cortices were then flattened between two glass slides separated by ~1 mm spacers and secured with lab tape. The tissue and slides were incubated overnight in 4% PFA in PBS, at which point the tissue was removed from between the slides and post-fixed in 30% sucrose for 16-24 h.

Tissue was embedded in Tissue-Tek OCT compound (Sakura) on dry ice and stored at -80 °C. For examining endogenous fluorescence (tdTomato from the AI14 line), 60 µm cryosections were freeze-mounted on Superfrost Plus slides. Slides were dried, washed twice for 5 min in PBS, incubated 10 min in 1:30,000 dilution of 5 mg/mL DAPI, washed 5 min in PBS, and coverslipped with Fluorogel (Electron Microscopy Sciences).

For immunostaining, 40 µm cryosections were collected in PBS and stored at 4 °C for up to 24 h or were collected in cryoprotectant solution (30% w/v sucrose, 30% v/v ethylene glycol, and 1% w/v PVP-40 in 0.1 M phosphate buffer) and stored at -20 °C for up to several weeks. Free floating sections were then incubated in the following solutions with gentle agitation at room temperature unless indicated: 3 X 10 min in PBS, 2-4 h in 10% normal donkey serum (NDS) in PBS + 0.3% Triton X-100 (PBST), 84-96 h in primary antibody in 5% NDS in PBST at 4 °C, 3 x 10 min in PBST, 2-3 h in secondary antibody in 5% NDS in PBST, 3 x 10 min in PBST, 10 min in 1:30,000 dilution of 5 mg/mL DAPI or 20 min in 1:1,000 dilution of 1 mM TO-PRO-3 (Invitrogen) in PBS, and 5 min in PBS. Sections were then mounted on slides and coverslipped with Fluorogel. The primary antibodies used were rabbit anti-Fos (1:10,000; Santa Cruz Biotechnology, Cat #sc-52), rabbit anti-GABA (1:5,000; Sigma, Cat #A2052), and mouse anti-NeuN (1:10,000; Millipore, Cat #MAB377). Secondary antibodies conjugated to Alexa 488 or Cy5 (Jackson Immunoresearch) were diluted 1:500 from 50% glycerol stocks.

Sections were imaged on Zeiss epifluorescence and 510 confocal microscopes. Consistent with prior observations for other fluorescent proteins (Kremers et al., 2009), we found that exposure of sections to some wavelengths of light, particularly in the ultraviolet range, caused red-to-green photoconversion of tdTomato. For red-and-green colocalization experiments, we avoided problems associated with this phenomenon by performing confocal imaging on sections that were not previously exposed to laser or epifluorescence illumination and by using TO-PRO3 for counterstaining rather than DAPI.

Images were processed in Photoshop and ImageJ to stitch multiple fields-of-view of single sections and to adjust contrast and brightness of each channel.

Data Analysis

For the time course experiment in the visual system, every fourth 60 µm coronal section through most of the rostral-caudal extent of V1 was imaged. The area of V1 in each section was outlined by hand, and the number of cells within that area was counted using custom-written automated software with manual correction. The number of TRAPed cells and the volume of V1 in the counted sections were summed across all sections for each animal, and the sums were used to

calculate the density of TRAPed cells in V1. The same approach was used to determine the density of TRAPed cells in the forelimb region of S1. The density of cells in each animal for both brain regions was normalized to the mean cell count for the respective regions in the dark group to produce the graphs in Figure 4D.

For the auditory experiment, every 40 μm coronal section through the entire rostral-caudal extent of the cochlear nuclei was imaged for all mice. One cochlear nucleus (right or left) for each mouse was randomly selected for quantitative analysis. TRAPed (red), Fos+ (green), and TRAPed Fos+ (yellow) cells in the DCN were counted manually, and their coordinates were recorded to calculate their positions along the dorsoventral axis of the nucleus. Granule cells both in the granule cell layer and in the core of the DCN were excluded from the analysis based on location and cell size due to their extensive processing of non-auditory information (Young and Oertel, 2004). Only sections in the middle 1/3 of the DCN along the rostral-caudal extent were included in the analysis of tonotopy, because these sections had roughly equal representations of both 4 kHz and 16 kHz stimuli as determined by Fos induction; due to the fact that the plane of sectioning was not perfectly orthogonal to the axis of tonotopy, more rostral sections included much of the 4 kHz representation, while more caudal sections included the representation of sounds 16 kHz and above. For the analysis of tonotopy, a line was drawn from the dorsal-most tip of the DCN to the ventral-most tip of the DCN; although this line extends to some extent in a ventrolateral to dorsomedial orientation, we defined this line as the dorsoventral axis for simplicity. The coordinates of individual cells were projected onto this axis to calculate their dorsoventral positions. The axis was divided into 20 evenly sized bins along its entire length, which differed to some extent between sections, and the numbers of cells in each bin were counted to produce the histograms in Figure 5C.

For the novel environment experiment, 60 uM coronal sections were collected. Subregions of the brain areas of interest were selected for quantification, and the equivalent subregions, identified by landmarks, were counted for every animal to get the raw values reported in Figures 6 and S6. In most cases, the experimenter was blind to the treatment of the animals. For quantification of cell densities in the blade analysis (Figure 6C), the areas of the granule cell layer in each blade were calculated by bisecting the genu and multiplying by the section thickness to determine the volume of tissue quantified.

SUPPLEMENTAL REFERENCES

Giorgi, C., Yeo, G.W., Stone, M.E., Katz, D.B., Burge, C., Turrigiano, G., and Moore, M.J. (2007). The EJC factor eIF4AIII modulates synaptic strength and neuronal protein expression. Cell *130*, 179-191.

Kobayashi, H., Yamamoto, S., Maruo, T., and Murakami, F. (2005). Identification of a cis-acting element required for dendritic targeting of activity-regulated cytoskeleton-associated protein mrna. Eur. J. Neurosci. *22*, 2977-2984.

Kremers, G.-J., Hazelwood, K.L., Murphy, C.S., Davidson, M.W., and Piston, D.W. (2009). Photoconversion in orange and red fluorescent proteins. Nat. Meth. *6*, 355-358.

Strominger, R.N., and Woolsey, T.A. (1987). Templates for locating the whisker area in fresh flattened mouse and rat cortex. J. Neurosci. Methods *22*, 113-118.

Wilson, T., and Treisman, R. (1988). Removal of poly(a) and consequent degradation of c-fos mrna facilitated by 3' AU-rich sequences. Nature *336*, 396-399.